

Evolution of binaries

Tomasz Bulik

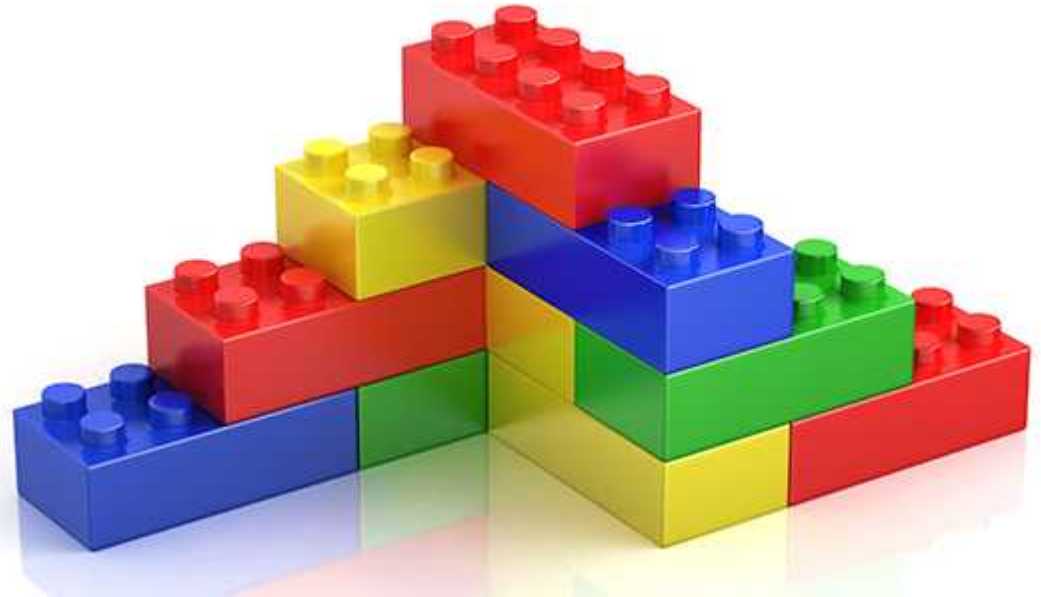
The plan July 24-28

Five lectures

Five tutorials

FOR TUTORIALS – PLEASE HAVE YOUR COMPUTERS READY!

Goal



Book:

- Peter Eggleton: Evolutionary Processes in Binary and Multiple Stars, Cambridge University Press, 2004.

Binary stars

Introduction

- What are they?
- How abundant ?

Measuring the stars

- Single stars
 - Spectra: temperature, surface gravity, chemical composition
 - Parallax → distance → Luminosity → Size
 - Accuracy - 25% ?

Visual binaries

- Long periods or nearby binaries
- What can be measured: P , e , i , a/D , inclination
- So also

$$\frac{GM}{D^3} \left(\frac{2\pi}{P} \right)^2 = \left(\frac{a}{D} \right)^3$$

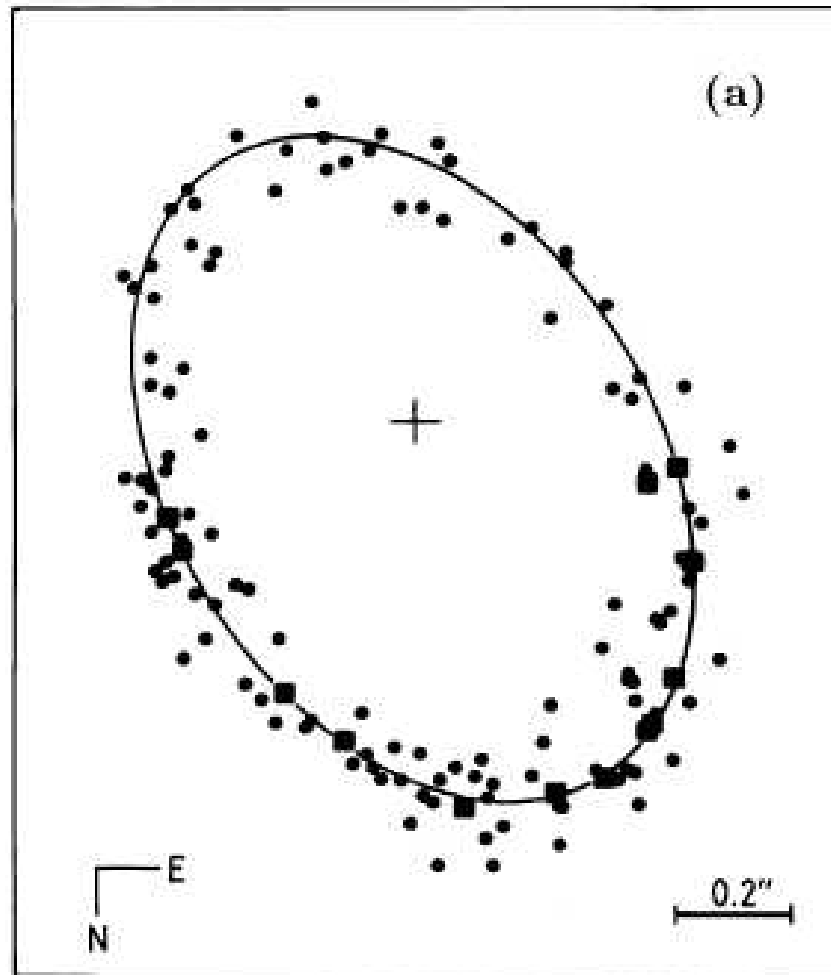
- D – from parallax?

Visual binaries

- Long periods or nearby binaries
- What can be measured: P , e , i , a/D , inclination
- So also

$$\frac{GM}{D^3} \left(\frac{2\pi}{P} \right)^2 = \left(\frac{a}{D} \right)^3$$

- D – from parallax?



An example of a visual binary
HR3579: $P=21.8$ lat, $e=0.15$, $a/D=0.66''$, $i=130^\circ$

Visual binaries

- Oscillations around their proper motion
- Common proper motion stars
- A list of all visual binaries – not a lot!

<http://www.dibonsmith.com/orbits.htm>

- More to come with GAIA!

Spectroscopic binaries

- Motion in spectroscopic data
- Line position variation with time
- What can be measured
 - Period
 - Radial velocity amplitude K
 - Ellipticity e
- Binaries with pulsars – an important subclass

Mass function

$$f_1 = \frac{M_2^3 \sin^3 i}{(M_1 + M_2)^2} = \frac{K_1^3 P (1 - e^2)^{3/2}}{2\pi G}$$

$$f_1 = 1.0385 \times 10^{-7} K_1^3 P (1 - e^2)^{3/2}$$

Minimal mass of the secondary

K in km/s,

P in days

F in solar masses

Determining the masses

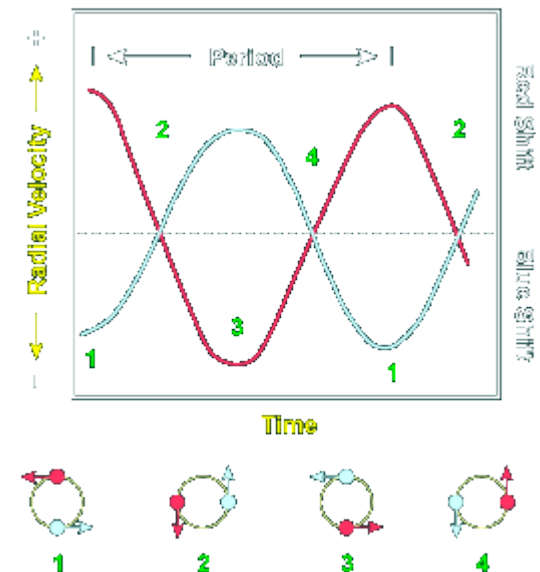
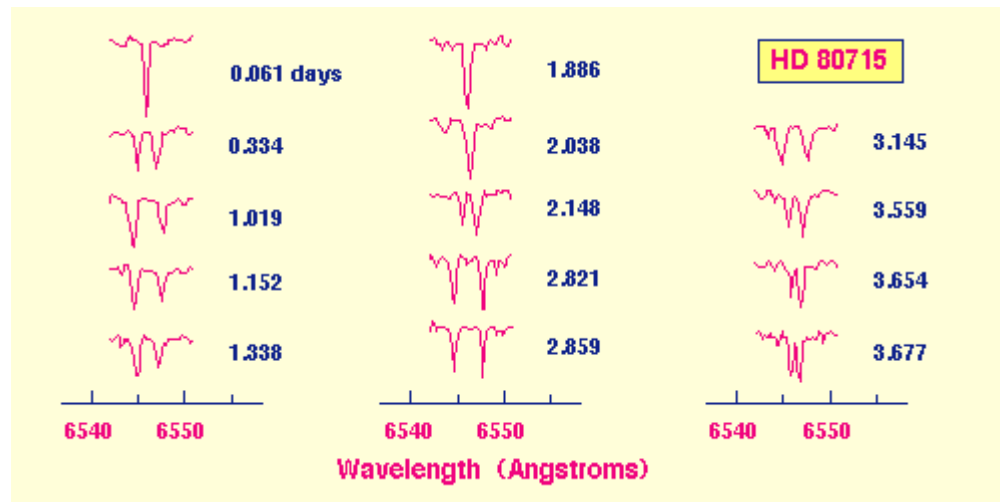
- Mean value of the angular factor
 - Integrate over the directions on a sphere
 - But not the entire one

$$M_1 \approx 1.25q(1 + q)^2 f_1$$

$$M_2 \approx 1.25(1 + q)^2 f_1$$

Double spectroscopic binaries

- Two mass functions
- Mass ratio
- If VB – We have inclination and distance!



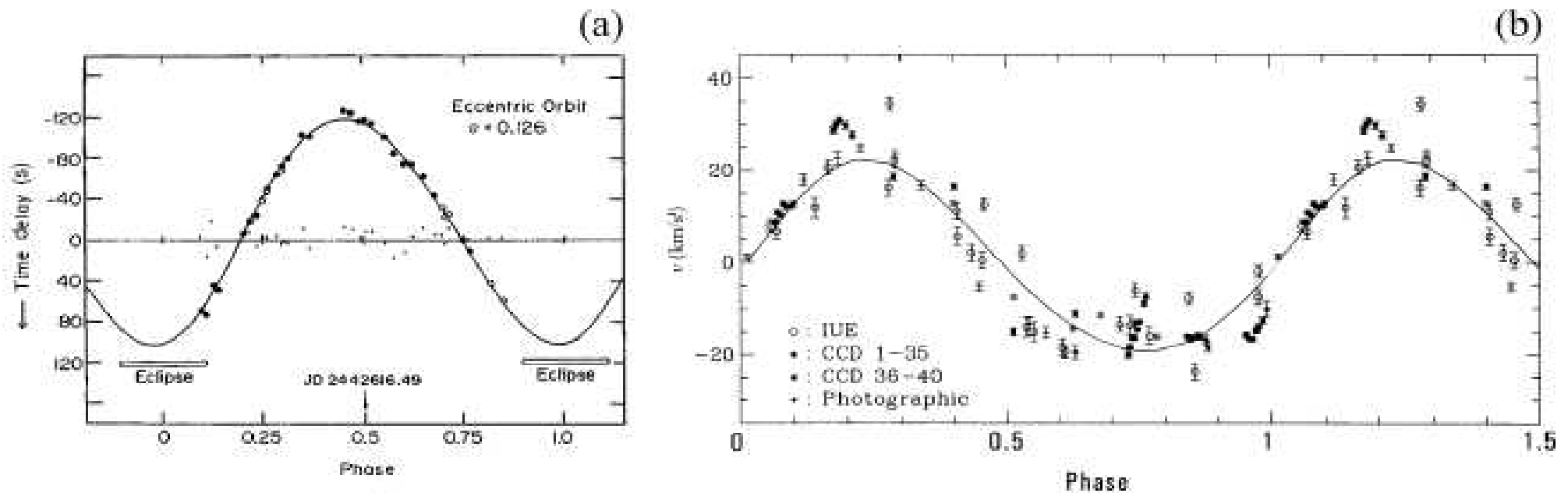


Figure 1.3 Radial velocity curves of both components of the massive X-ray binary Vela X-1 (GP Vel). (a) Doppler shift of the pulses of the X-ray pulsar: note the accurate fit to the Keplerian curve ($P = 8.964$ days, $e = 0.126$, $f_1 = 18.5 M_{\odot}$). Small dots near the axis are the residuals multiplied by 2. (b) Doppler shift of absorption lines in the visible spectrum: note the larger scatter, due to irregular pulsations. From these lines $f_2 \sim 0.013$. The ratio f_2/f_1 is the cube of the mass ratio q (~ 0.09). (a) is from Rappaport *et al.* (1976), (b) from van Kerkwijk *et al.* (1995b).

Pulsars – GR corrections

- Periastron shift

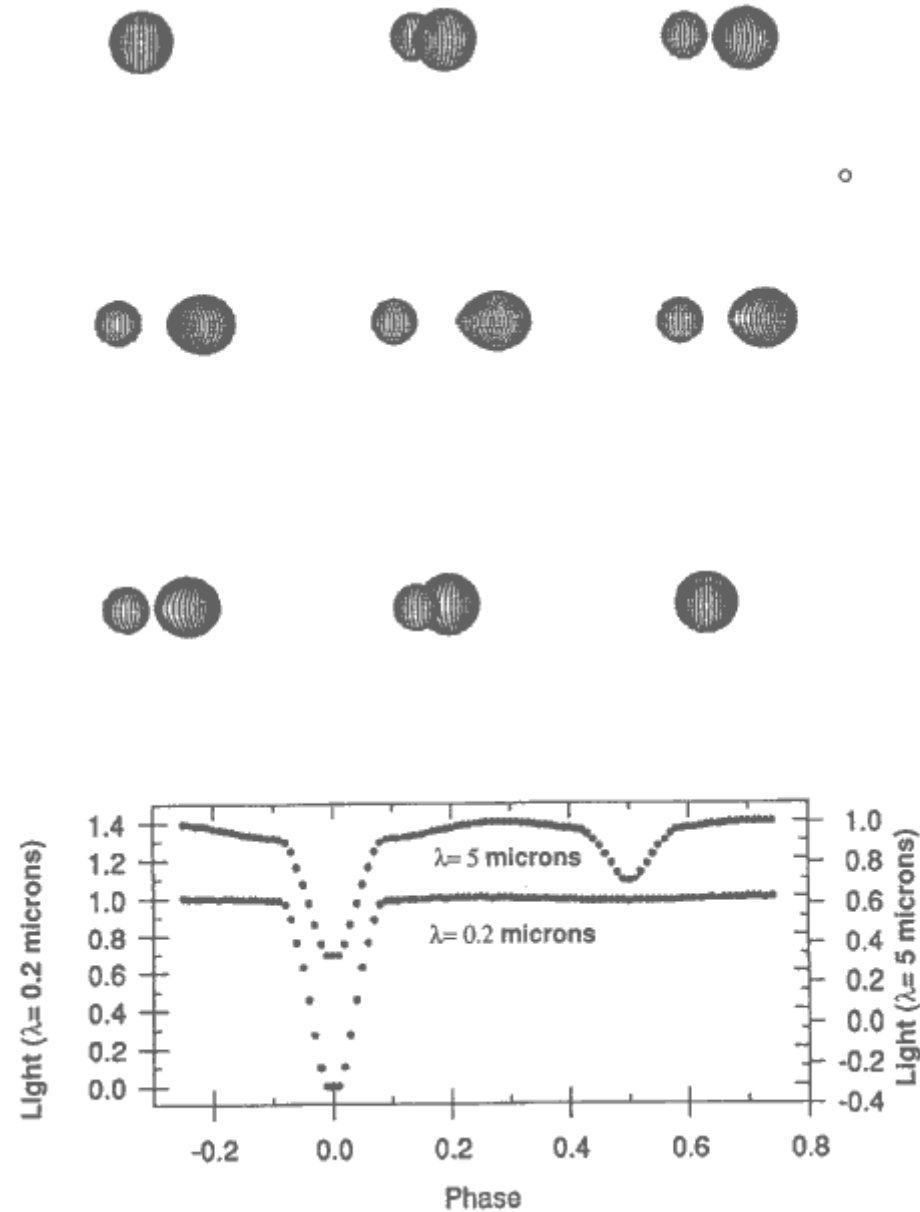
$$Z_{GR} = \frac{3GM}{c^2 a(1 - e^2)} \frac{2\pi}{P}$$

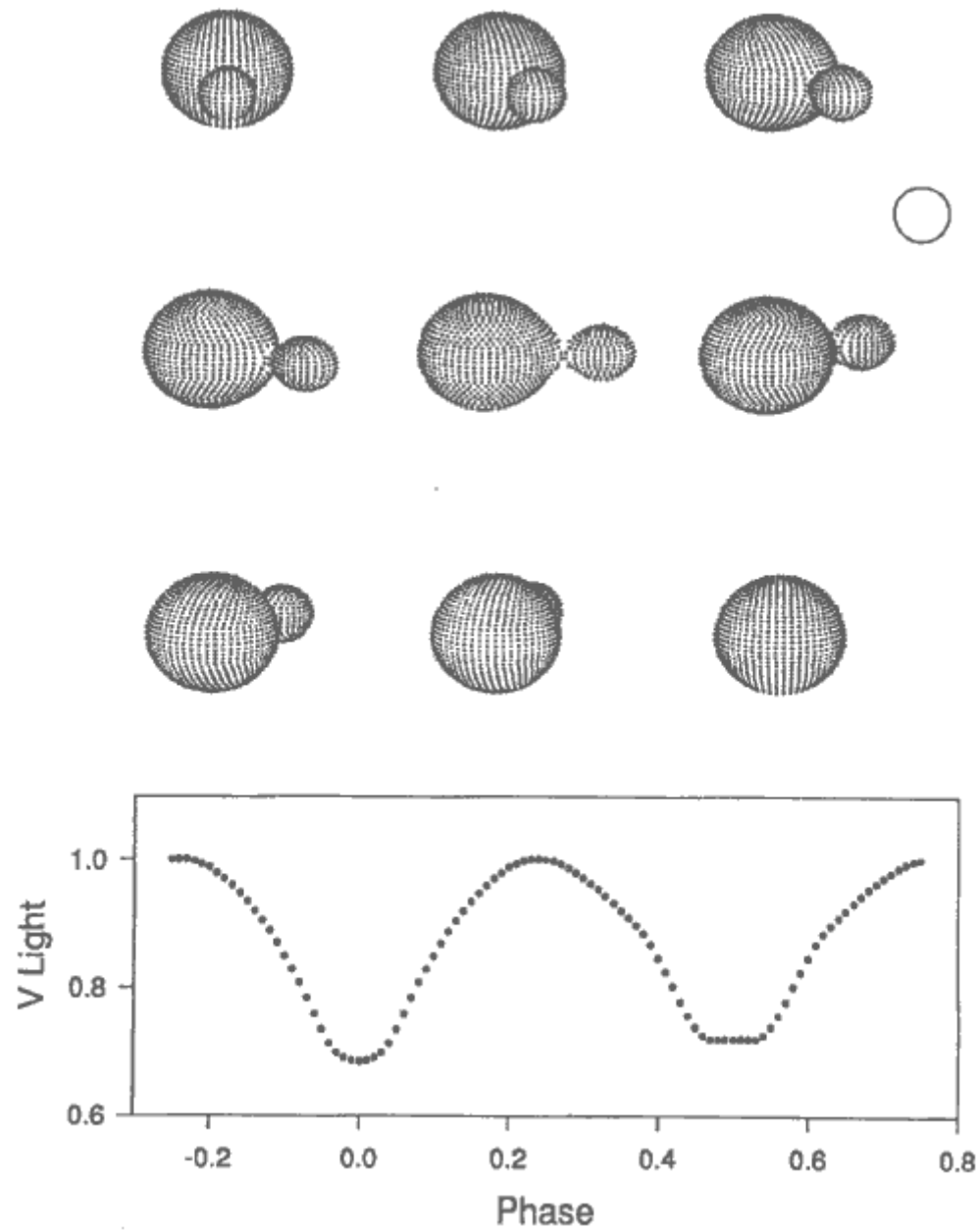
- Gamma (doppler + gravitational redshift):

$$\gamma = \frac{G(M_1 + 2M_2)e}{c^2 M} \frac{P}{2\pi}$$

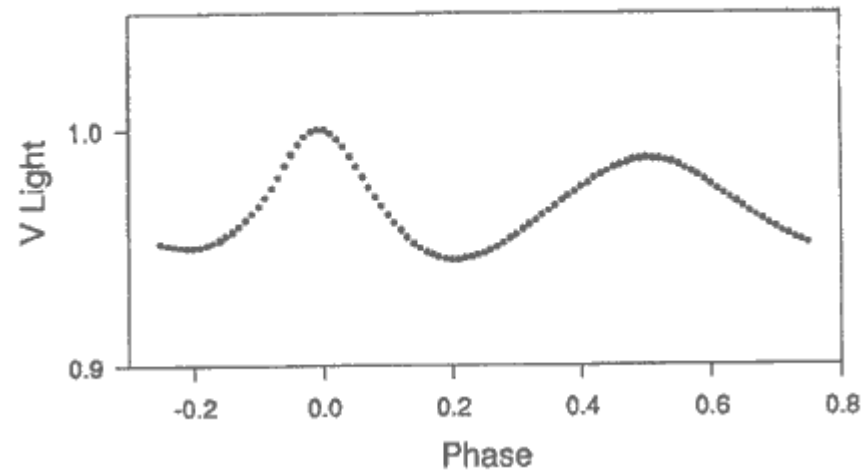
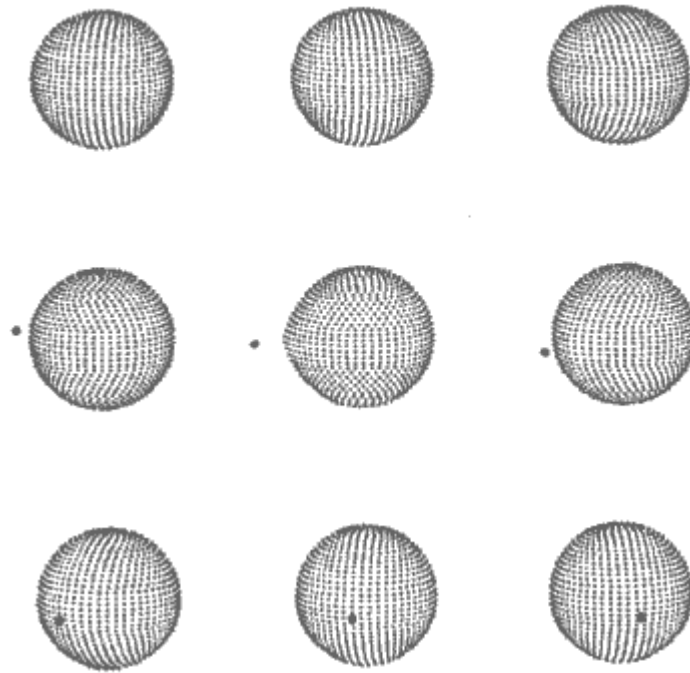
- Plus additional 3 parameters
- Full solution

Photometric binaries

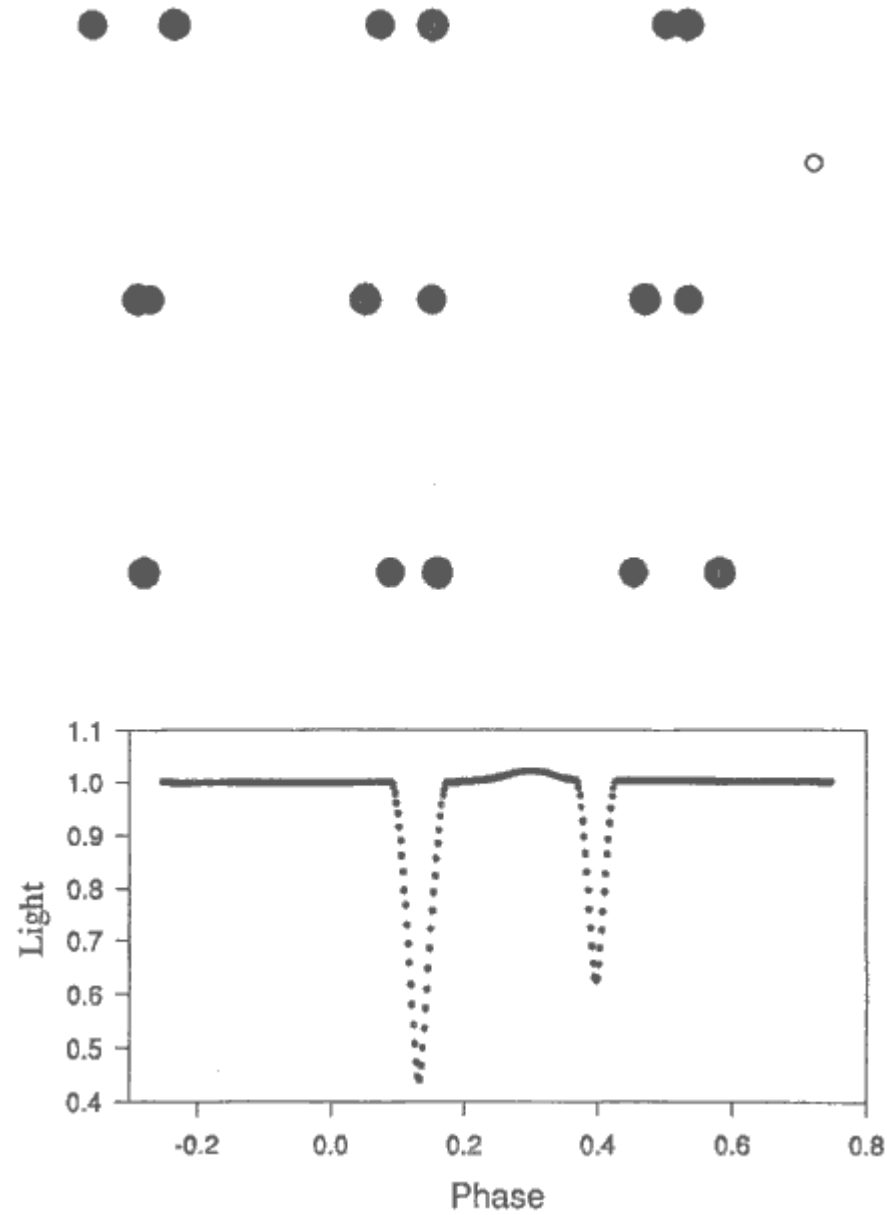




<http://www.tass-survey.org/tass/refs/wilson/index.html>



<http://www.tass-survey.org/tass/refs/wilson/index.html>



<http://www.tass-survey.org/tass/refs/wilson/index.html>

Photometric binaries

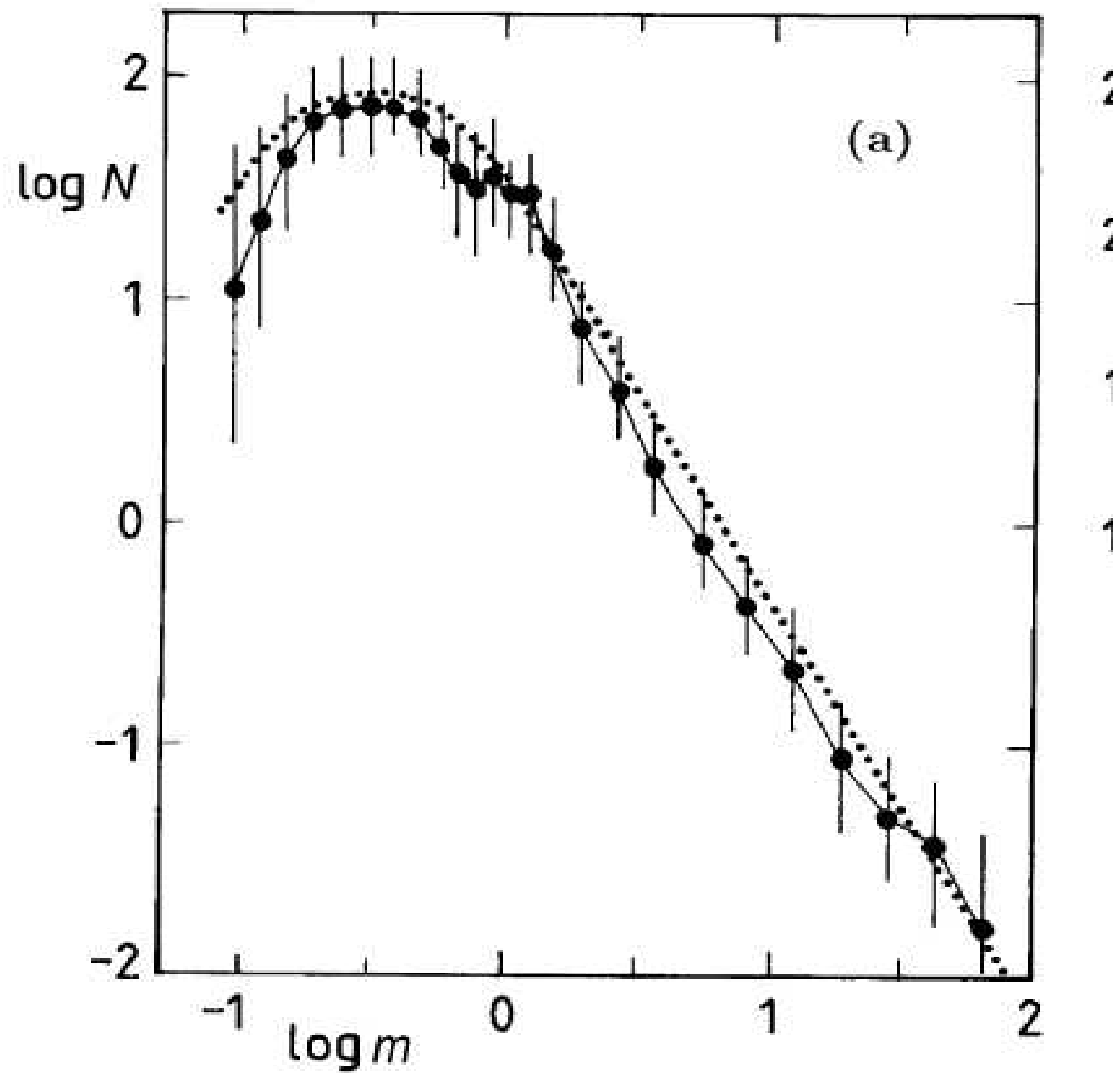
- Periodic change of the radiation intensity in a given band
 - eclipses
 - deformations
 - disks
- What can be measured: P , e , i , R_1/A , R_2/A ,
- Component temperatures

The ESB2 binaries

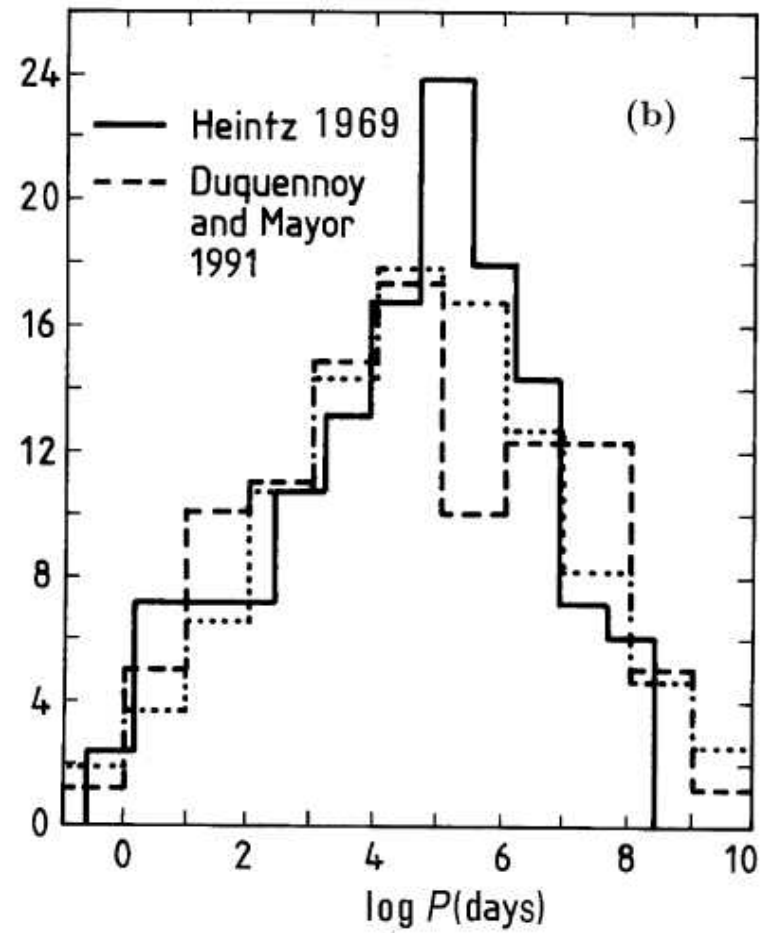
- Eclipsing
- Doubly spectroscopic \rightarrow two mass functions
- Determine temperatures: $T_1, T_2, P, e, i \rightarrow A$
- Eclipses $\rightarrow R_1/A, R_2/A \rightarrow R_1, R_2$
- $T + R \rightarrow L \rightarrow D$!
- Independent distance determination !

The statistics of binaries

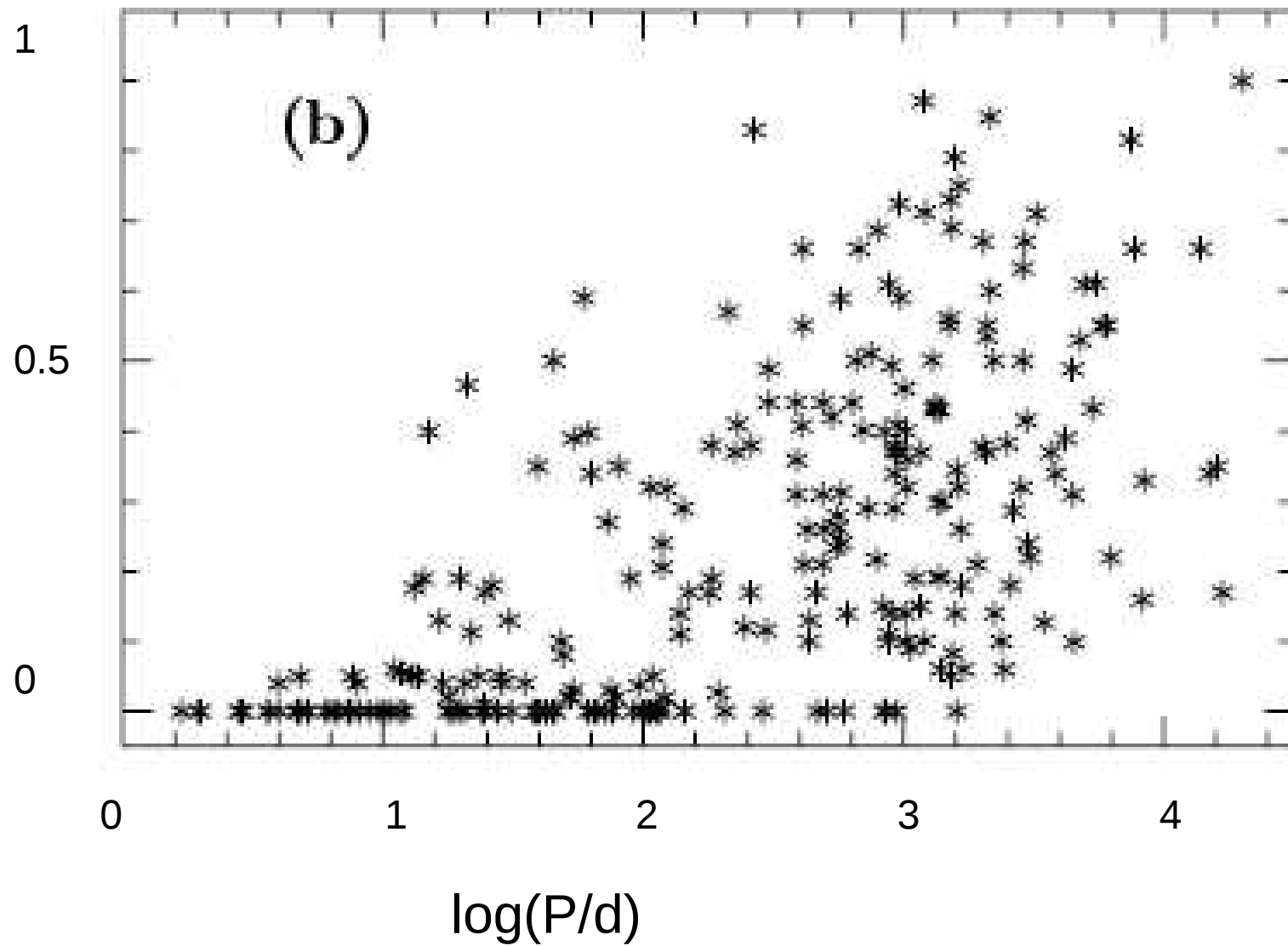
- Mass distributions
 - Primary mass
 - Mass ratio
- Orbital parameters
 - Periods: break around 30-300 lyrs?
 - ellipticities



Orbit distribution



Ellipticities



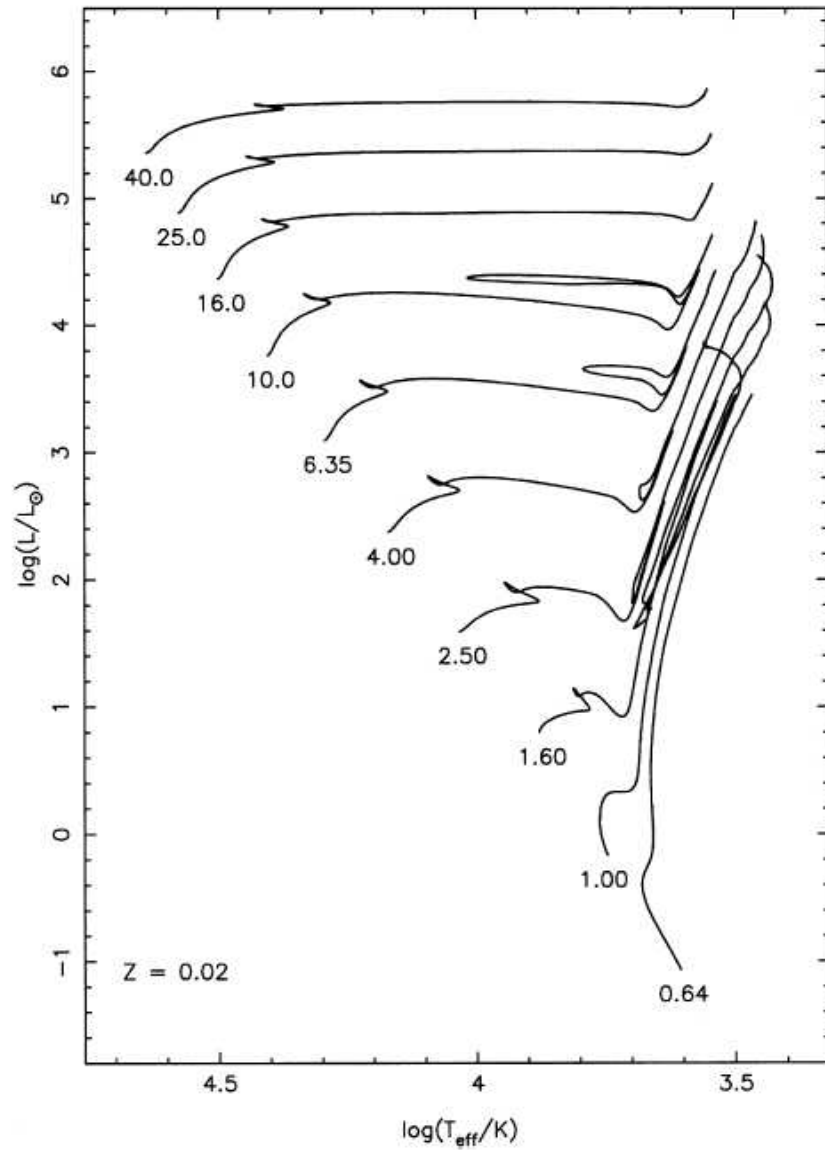


Figure 1. Selected OVS evolution tracks for $Z = 0.02$, for masses 0.64, 1.0, 1.6, 2.5, 4.0, 6.35, 10, 16, 25 and $40 M_{\odot}$.

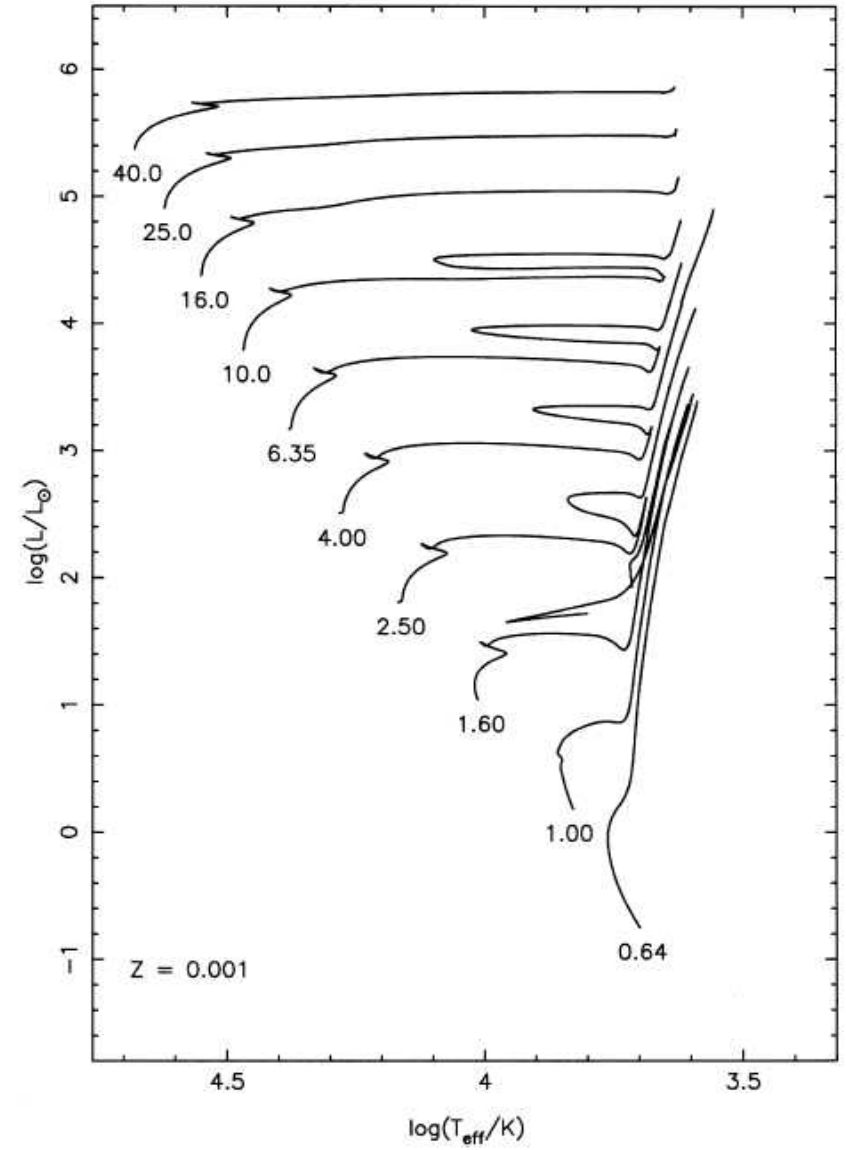


Figure 2. Same as Fig. 1 for $Z = 0.001$. The $1.0 M_{\odot}$ post-helium flash track has been omitted for clarity.

Main sequence

$$L = \frac{0.397M^{5.5} + 8.53M^{11}}{0.000255 + M^3 + 5.45M^5 + 5.56M^7 + 0.789M^8 + 0.00587M^{9.5}}$$

$$R = \frac{1.715M^{2.5} + 6.6M^{6.5} + 10.09M^{11} + 1.0125M^{19} + 0.0745M^{19.5}}{0.01077 + 3.082M^2 + 18.85M^{8.5} + M^{18.5} + 0.000226M^{19.5}}$$

Temperature – the SB law.

Main sequence time

$$t_{MS} = \frac{1532 + 2740M^4 + 146M^{5.5} + M^7}{0.0397M^2 + 0.3432M^7}$$

After the main sequence

$$M_c = \frac{0.11M^{1.2} + 0.0022M^2 + 9.6 \times 10^{-5}M^4}{1 + 0.0018M^2 + 1.75 \times 10^{-4}M^3}$$

Hertzsprung gap - and then Hayashi track

$$R_{HT} = (1.65L^{0.47} + 0.17L^{0.8})M^{-0.31}$$

Stellar radii

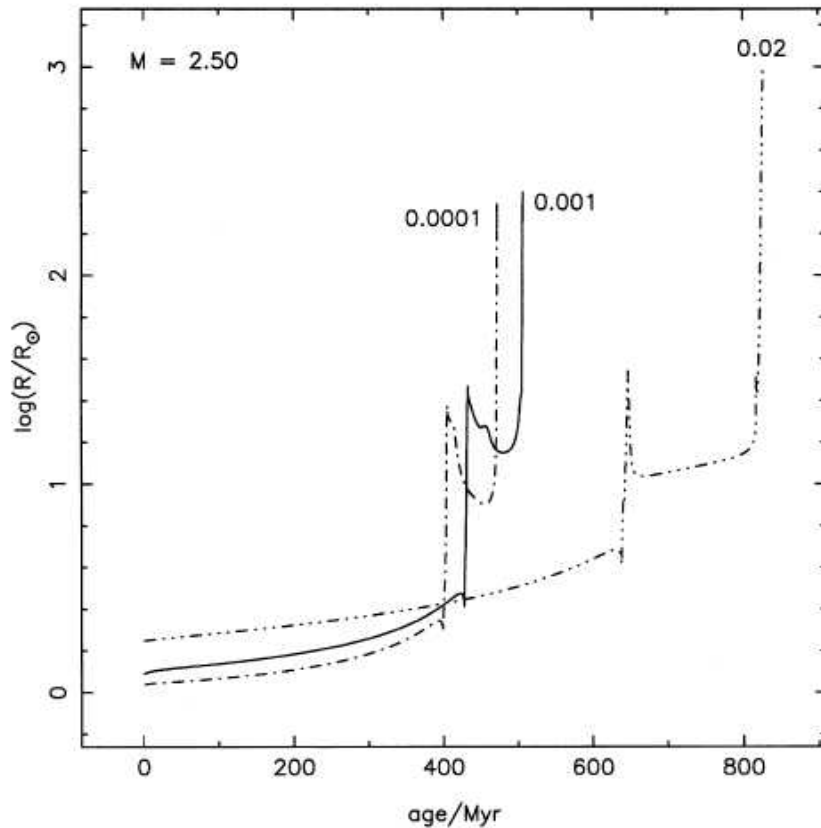


Figure 4. Radius evolution as a function of stellar age for $M = 2.5 M_{\odot}$, for metallicities 0.0001, 0.001 and 0.02. Tracks are from the detailed models, and run from the ZAMS to the point of termination on the AGB.

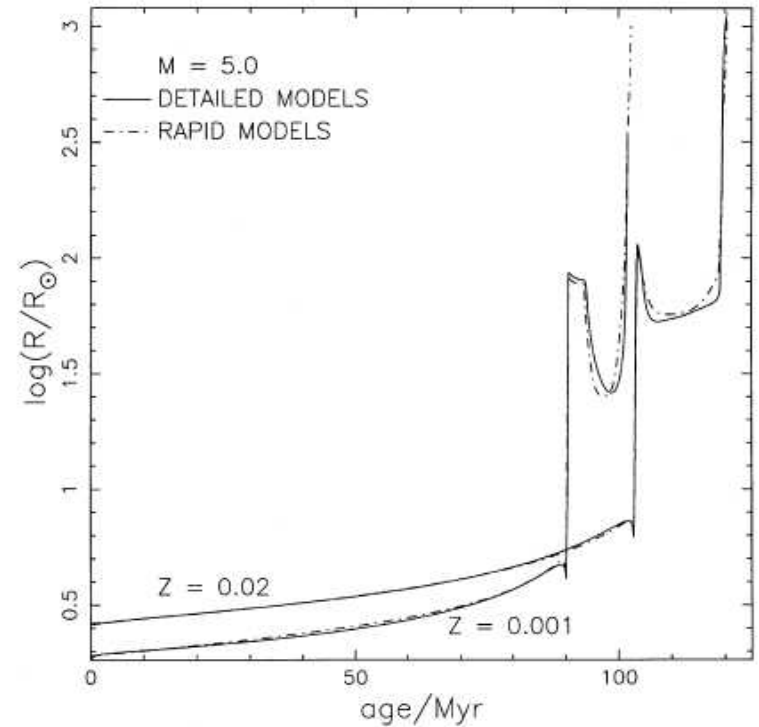


Figure 13. Radius evolution from the ZAMS to the end of the AGB for a $5.0 M_{\odot}$ star, for metallicities 0.001 and 0.02, showing the detailed model points (solid lines) and the fitted tracks (dot-dashed lines).

Stellar winds

- Mass dependence
- Metallicity dependence
- Very important for evolved stars

Helium stars

$$L = \frac{1000M^{10}}{0.0012 + 1.08M^5 + 2.63M^7 + 0.142M^{8.5}}$$

$$R = \frac{M^2 + 0.1M^3}{0.36 + 3.24M + 1.75M^2}$$

$$t_{HeMS} = \frac{2.985 + 51.88M^6 + 43.95M^{7.5} + M^9}{0.3596M^4 + 6.217M^{9.5}}$$

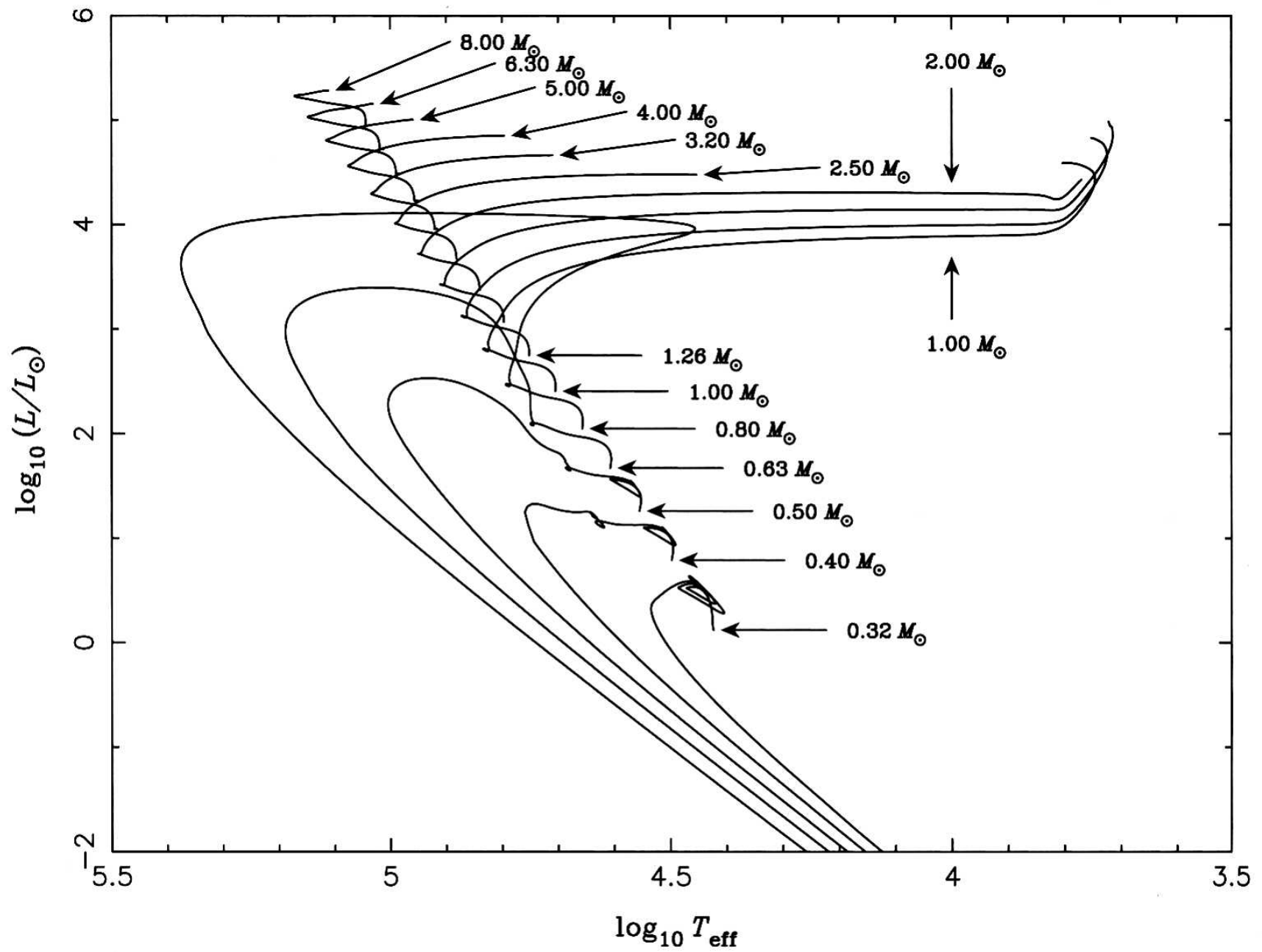


Figure 2.18 The theoretical HR diagram for He stars. Low-mass stars ($M \lesssim 0.63 M_{\odot}$) evolve to white dwarfs without going to the red-giant region. Those of intermediate mass ($0.8\text{--}2.0 M_{\odot}$) evolve to red giants, and those of $M \gtrsim 2.5 M_{\odot}$ reach a supernova explosion while still very blue (Courtesy of Z. Han).

End product – compact object

Excepr for secial cases

Mass and type depend on:

metallicity
wiinds
Rotation?

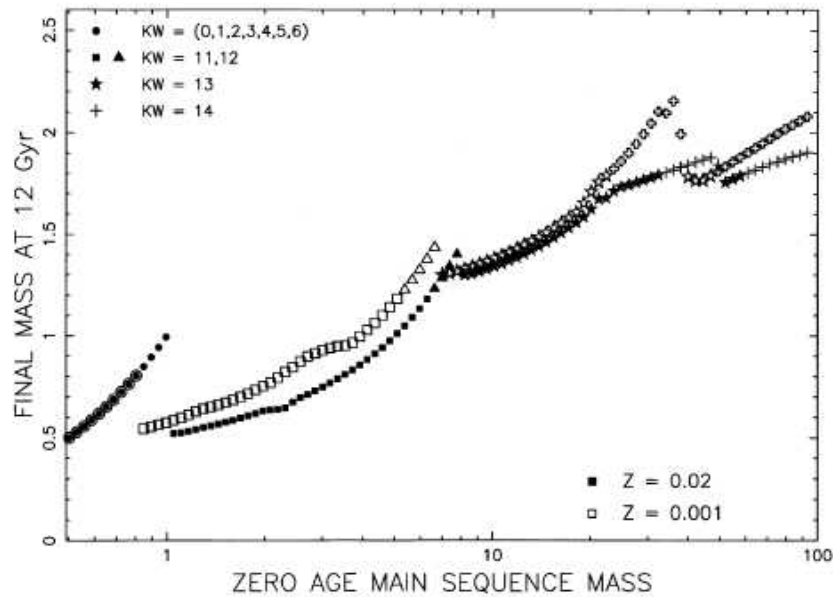


Figure 20. Distribution of remnant masses and types after 1.2×10^{10} yr of evolution, as a function of initial mass, for $Z = 0.001$ (hollow symbols) and $Z = 0.02$ (filled symbols).

White dwarfs

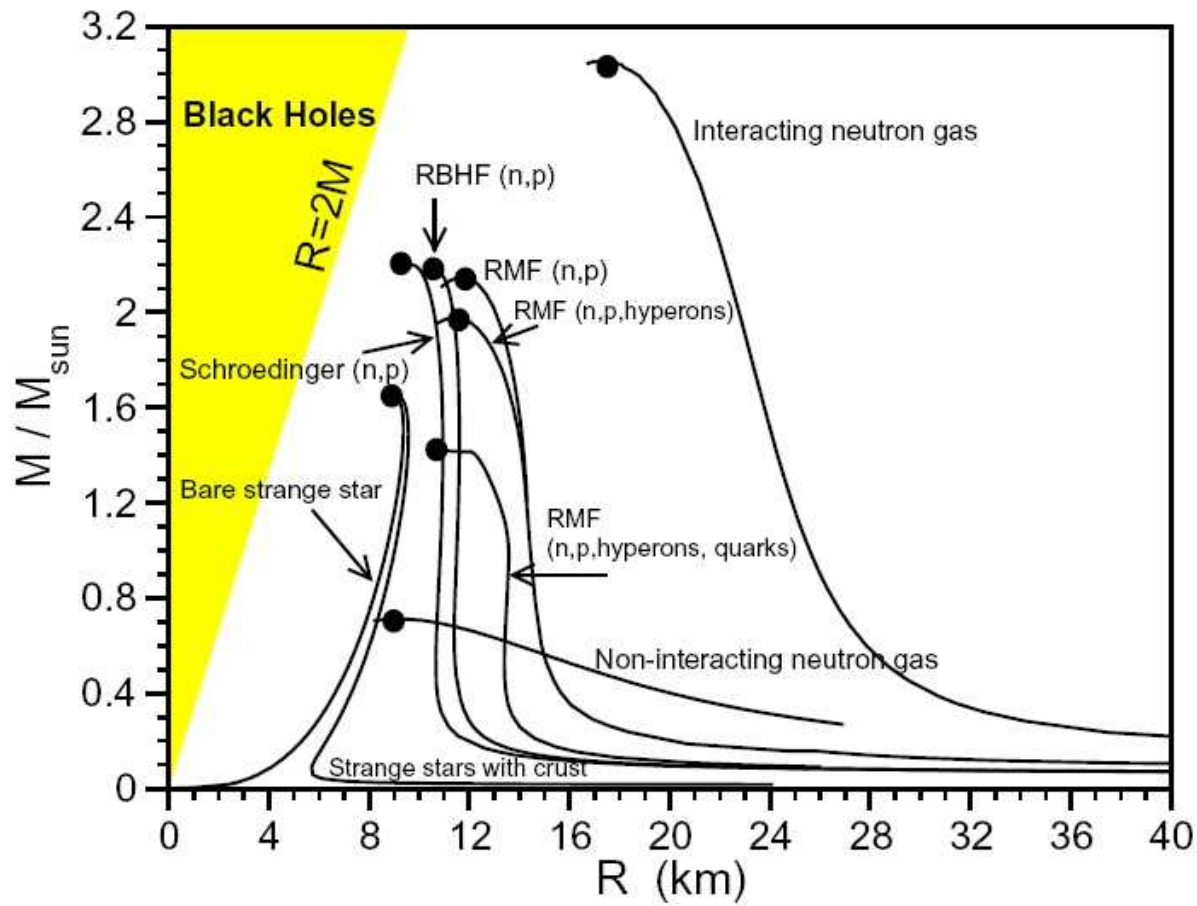
$$R = R_{Ch} \left[\left(\frac{M_{Ch}}{M} \right)^{\frac{2}{3}} - \left(\frac{M}{M_{Ch}} \right)^{\frac{2}{3}} \right]^{\frac{1}{2}} \left[1 + 3.35 \left(\frac{M_{pl}}{M} \right)^{\frac{2}{3}} + \frac{M_{pl}}{M} \right]$$

$$R_{Ch} = 0.0228 \langle Z/A \rangle R_{\odot}$$

$$M_{Ch} = 5.83 \langle Z/A \rangle^2 M_{\odot}$$

$$M_{pl} = 0.0016 \langle Z/A \rangle^{3/2} \langle Z^2/A \rangle^{3/4} M_{\odot}$$

Neutron stars



(Weber et al. ArXiv: 0705.2708)

Black holes

- Practically point masses
- Gravitational radius $R=2M$
- Marginally stable orbit $R=6M$

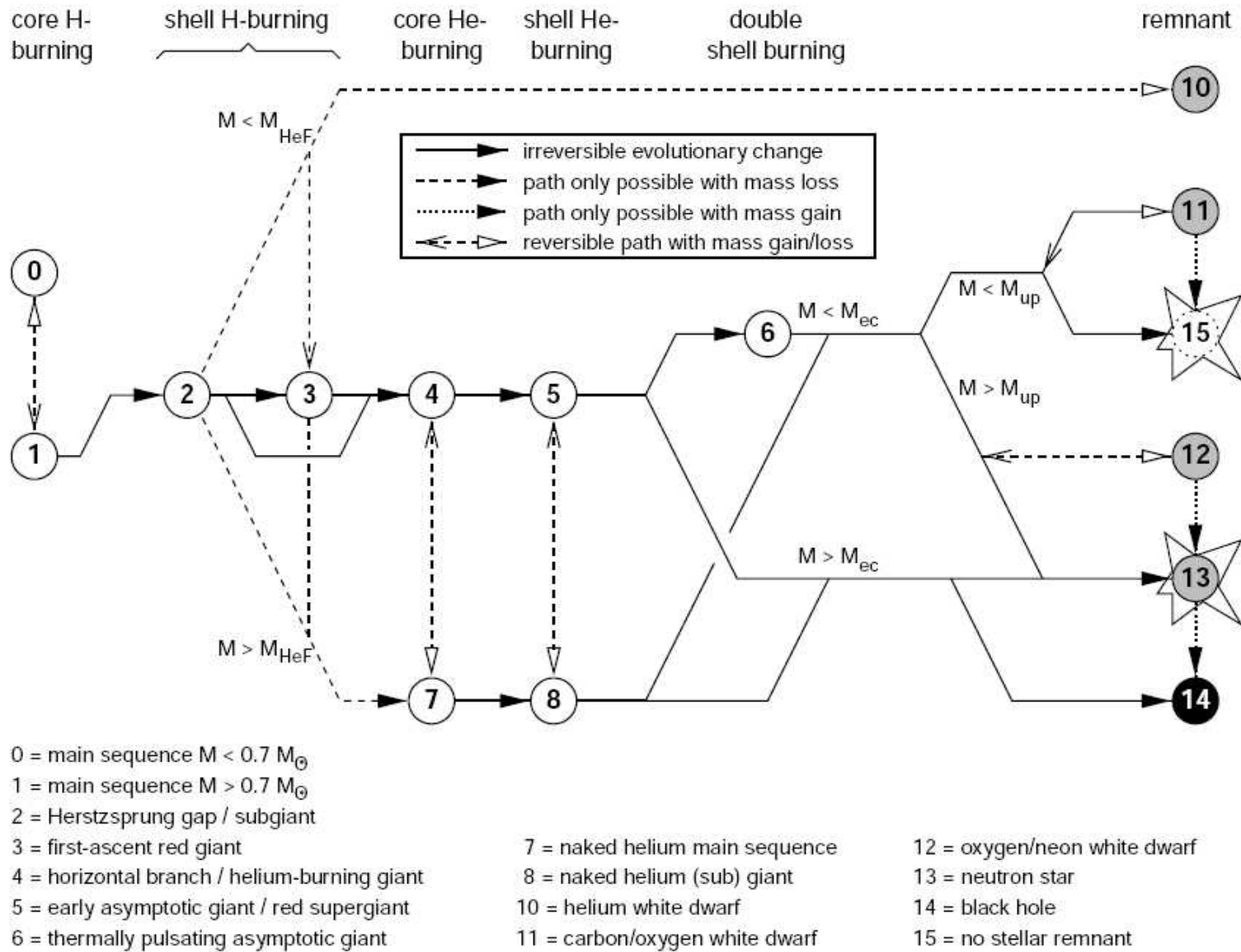


Figure 19. Possible evolution paths through the various stellar evolution phases.

Time scales – single and binary stars

- Nuclear
- Thermal (Kelvin Helmholtz)
- Dynamical
- Orbital

Dynamical timescale

Free fall if pressure disappears:

$$\frac{d^2 R}{dt^2} = -\frac{GM}{R^2} \quad R(t=0) = R_{\odot}, \quad \dot{R}(t=0) = 0$$

$$t = \frac{\pi}{\sqrt{8}} \sqrt{\frac{R_{\odot}^3}{GM}} \approx 1600 \text{ s}$$

Kelvin Helmholtz timescale

Radiating gravitational binding energy with current luminosity

$$t \approx \frac{\left(\frac{GM_{\odot}^2}{R_{\odot}} \right)}{L_{\odot}} \approx 3 \times 10^7 \text{ years}$$

Nuclear timescale

Converting mass into energy via nuclear reactions

P-p cycle efficiency – 0.7%

Only about 1% of H converted

$$t = \frac{f \times M_{\odot} c^2}{L_{\odot}} \approx 10 \text{Gyrs}$$

Scaling:

$$t(M) \approx 10 \text{Gyrs} \left(\frac{M_{\odot}}{M} \right)^2$$

Binaries

T Bulik

Energy and angular momentum

Energy in the CM system

$$E = \frac{1}{2}\mu\dot{r}^2 - \frac{GM_1M_2}{r}$$

$$\frac{E}{\mu} = \frac{\dot{r}^2}{2} - \frac{GM}{r}$$

Angular momentum in the CM sysem

$$\vec{J} = \mu\vec{r} \times \dot{\vec{r}}$$

$$\frac{J}{\mu} = \sqrt{GMA(1 - e^2)}$$

Orbit parameters

Trajectory:

$$r = \frac{p}{1 + e \cos(\varphi - \varphi_0)}$$

$$p = \frac{J^2}{GM_1 M_2 \mu}$$

$$e = \sqrt{1 + \frac{2Ep}{GM_1 M_2}}$$

Orbits

Kepler law

$$\left(\frac{2\pi}{P}\right)^2 A^3 = G(M_1 + M_2)$$

Angular momentum

$$J = \frac{M_1 M_2}{M_1 + M_2} \frac{2\pi A^2 \sqrt{1 - e^2}}{P}$$

Teorem of rigid rotation

*For a given mass distribution the lowest energy state corresponds to the rigid rotation
eg.. Lynden-Bell & Pringle (1974) MNRAS*

$$T = \frac{1}{2} \int v^2 \rho dV = \frac{1}{2} \int v^2 dm$$

$$J = \int R v_\phi dm$$

$$I = \int R^2 dm$$

$$(a_1 b_1 + \cdots + a_n b_n)^2 \leq (a_1^2 + \cdots + a_n^2)(b_1^2 + \cdots + b_n^2).$$

$$I \int v_{\phi}^2 dm = \int R^2 dm \int v_{\phi}^2 dm \geq \left[\int R v_{\phi} dm \right]^2$$

so

$$T = \frac{1}{2} \int v^2 dm \geq \frac{1}{2} \int v_{\phi}^2 dm \geq \frac{1}{2} \frac{J^2}{I}$$

Motion around z axis

Rigid rotation

Rigid rotation corresponds to the lowest energy.

Circularization

- Tight systems have low eccentricity
- Rotation periods – tough to measure, but close to the orbital period.
- Time scales

$$t_{sync} \propto A^6$$

$$t_{circ} \propto A^8$$

Mass loss through winds

Circular orbits and spherical wind

$$dJ = \omega r_1^2 dM_1 + \omega r_2^2 dM_2$$

$$\omega = \frac{2\pi}{P} \quad r_1 = A \frac{M_2}{M_1 + M_2}$$

$$dJ = J \left[\frac{M_2}{M_1 + M_2} \frac{dM_1}{M_1} + \frac{M_1}{M_1 + M_2} \frac{dM_2}{M_2} \right]$$

But one can use the definition

$$\frac{dJ}{J} = \frac{dM_1}{M_1} + \frac{dM_2}{M_2} - \frac{1}{2} \frac{d(M_1 + M_2)}{M_1 + M_2} + \frac{1}{2} \frac{dA}{A}$$

Orbit change due to mass loss

$$\frac{dA}{A} = -\frac{d(M_1 + M_2)}{M_1 + M_2} \quad -\frac{d(M_1 + M_2)}{M_1 + M_2} = \frac{1}{2} \frac{dP}{P}$$

Czyli

$$\frac{P}{P_0} = \left(\frac{M_{1_0} + M_{2_0}}{M_1 + M_2} \right)^2$$

Wind mass loss causes orbits to expand and the period grows as inverse mass square

Roche lobe

$$\Phi_1 = -\frac{GM_1}{\sqrt{(x - A_1)^2 + y^2 + z^2}}$$

$$\Phi_2 = -\frac{GM_2}{\sqrt{(x + A_2)^2 + y^2 + z^2}}$$

$$\Phi = \Phi_1 + \Phi_2 - \frac{1}{2}\Omega_B^2(x^2 + y^2)$$

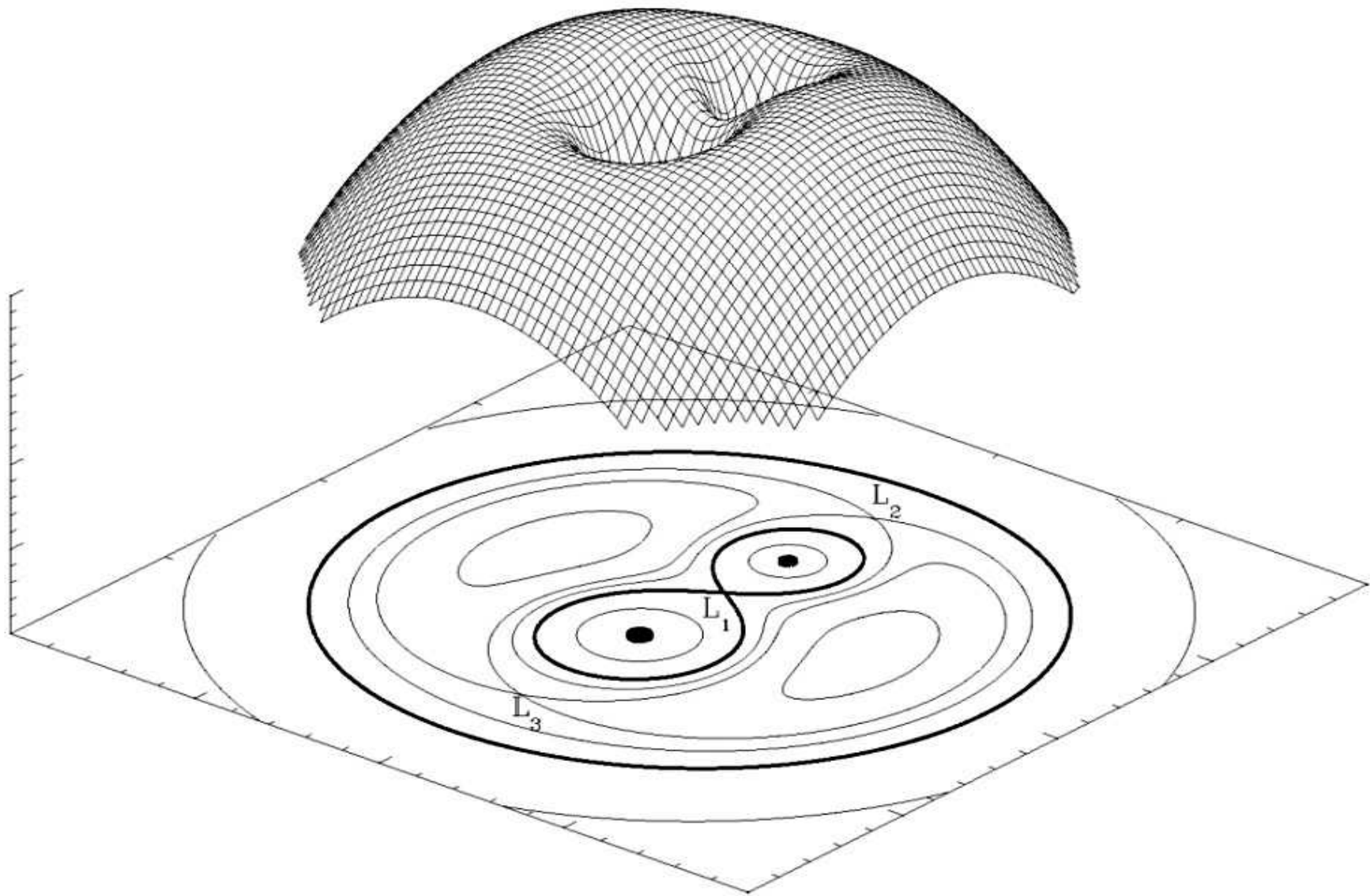
Roche lobe

$$\Phi_1 = -\frac{GM_1}{\sqrt{(x - A_1)^2 + y^2 + z^2}}$$

$$\Phi_2 = -\frac{GM_2}{\sqrt{(x + A_2)^2 + y^2 + z^2}}$$

$$\Phi = \Phi_1 + \Phi_2 - \frac{1}{2}\Omega_B^2(x^2 + y^2)$$

Coriolis force neglected



R_c – radius of the sphere with the volume equal to the Roche lobe volume

R_c – what does it depend on ?

Approximations $\frac{R_L}{A} = x_L(q)$

$$\frac{R_L}{A} = \frac{2}{3^{4/3}} (1 + q)^{-1/3}$$

Kopal 1955

Paczyński 1971

$$\frac{R_L}{A} = \frac{2}{3^{4/3}} \left(\frac{q}{1 + q} \right)^{1/3}$$

$$\frac{R_L}{A} = \frac{0.49q^{2/3}}{0.6q^{2/3} + \ln(1 + q^{1/3})}$$

$$\frac{R_L}{A} = 0.44 \frac{q^{0.33}}{(1 + q)^{0.2}}$$

Eggleton 1983

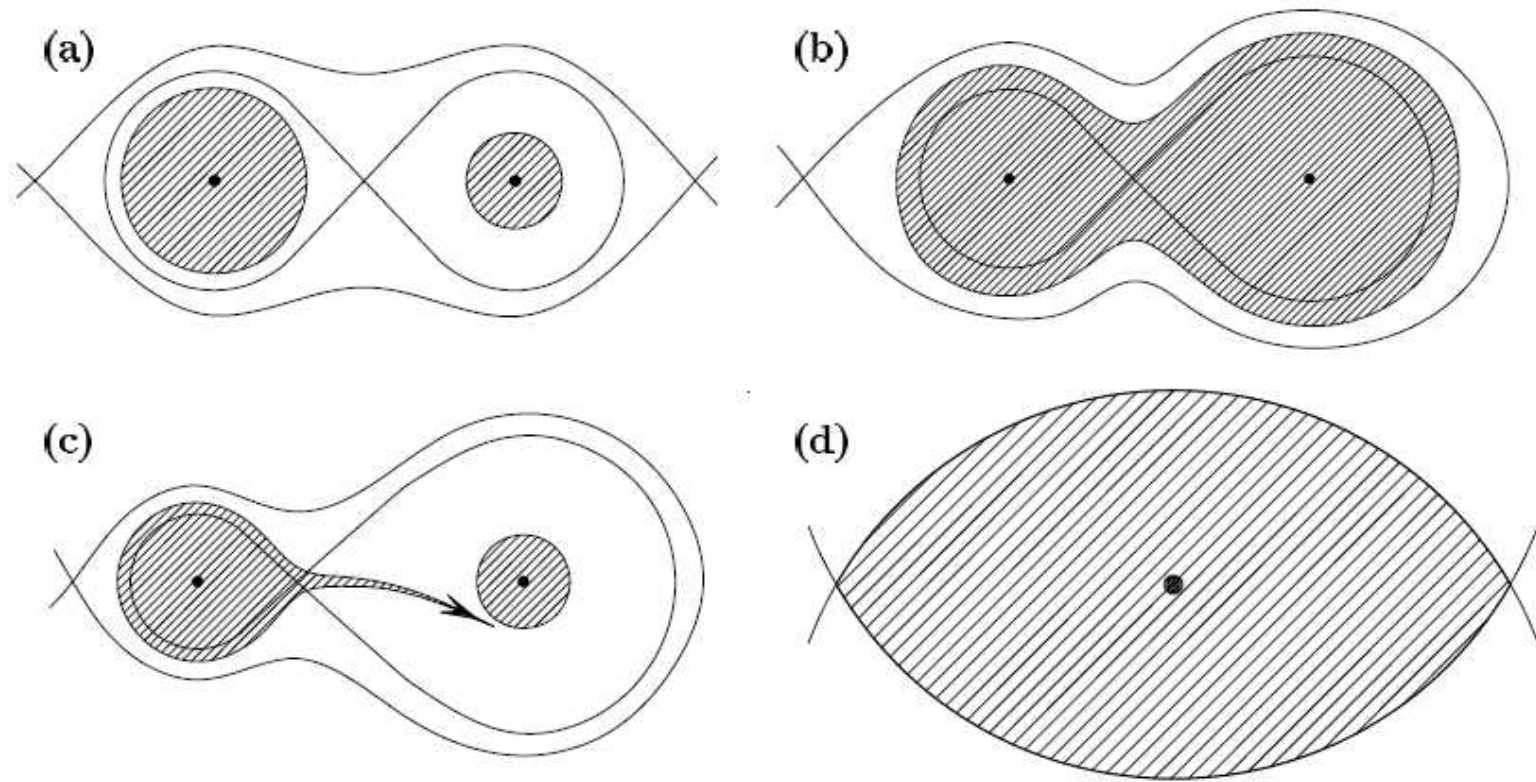


Figure 3.1 Some equipotential surfaces of the Roche potential – Eq. (3.2). For each of four different mass ratios ($q = 1, 2, 4, \infty$, *1 being to the right) the critical equipotentials passing through the inner and outer neutral points are indicated; some other equipotentials are also sketched. The case $q = \infty$ (d) has a neutral point all round the equator. A star can be in hydrostatic equilibrium only if it fills a closed equipotential surface, as in (a), (b) and (d). The left-hand star in (c) is unstable, and material flows towards the companion, being deflected by the Coriolis force. In (d), the rotation axis is in the plane of the paper, but in (a)–(c) it is perpendicular to the plane of the paper, in an anticlockwise sense.

Period when filling the Roche lobe

$$\frac{R_L}{A} = \frac{2}{3^{4/3}} (1 + q)^{-1/3}$$

$$\frac{GM}{A^3} = \left(\frac{2\pi}{P} \right)^2$$

$$P_{cr} = \left(\frac{3\pi}{G\bar{\rho}} \right)^{1/2} \left(\frac{q}{1+q} \right)^{1/2} x_L^{-3/2}$$

$$M = \frac{q+1}{q} M_1$$

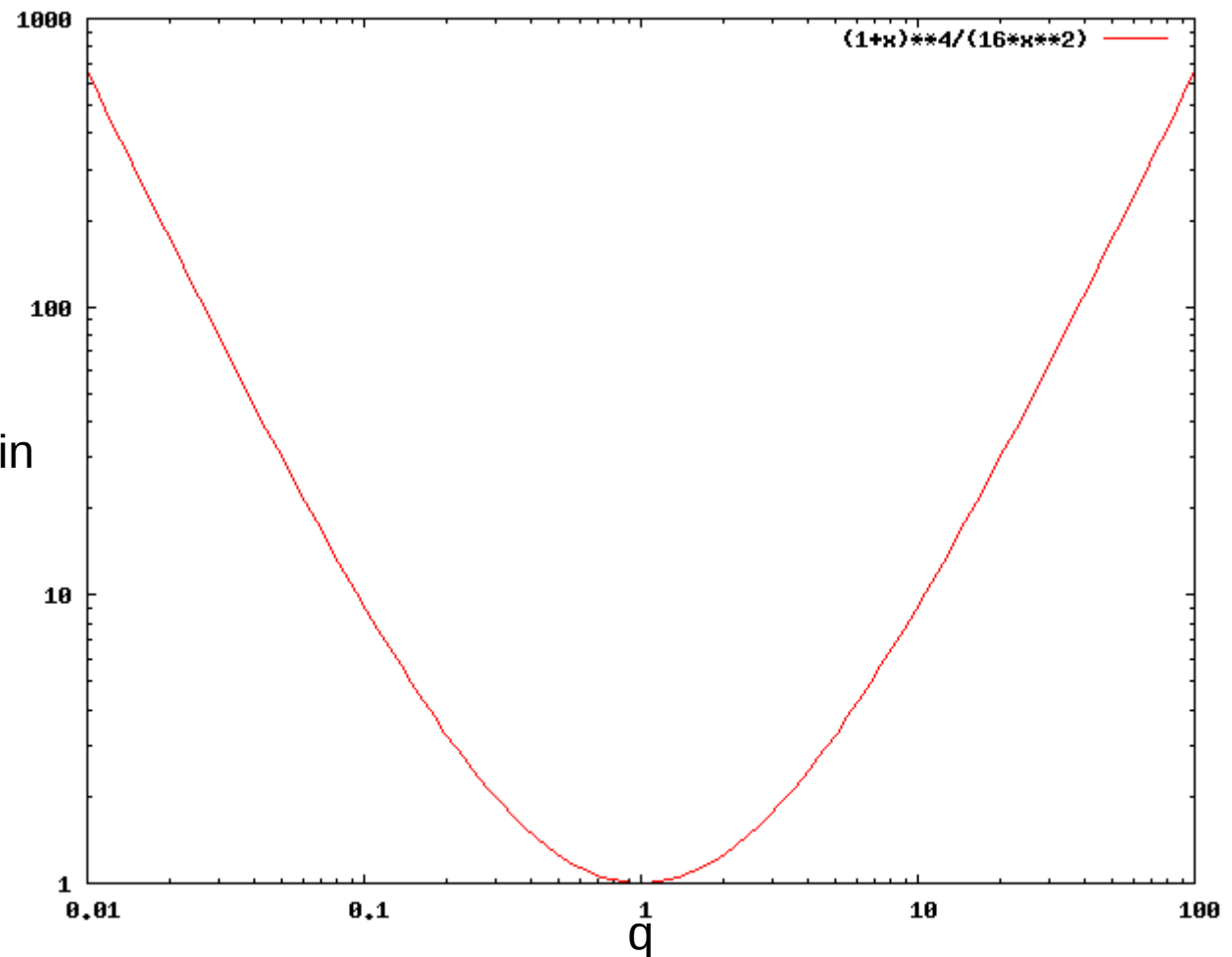
Weak dependence on q

Conservative mass transfer

$$A = \frac{J^2}{G} \frac{M}{M_1^2 M_2^2} = A_{min} \frac{(1+q)^4}{16q^2}$$

Minimum at $q=1$.

A/A_{min}



In conservative mass transfer the system tightens when mass flows from the more massive component while it expands of the donor is less massive component.

Consequences for mass transfer stability

Angular momentum loss mechanisms

- Mass loss in winds
- Mass loss – magnetic breaking
- Mass loss through L2

-

$$\frac{dJ}{dM} = \alpha \frac{J}{M}$$

- Gravitational waves

$$\frac{1}{J} \frac{dJ}{dt} = -\frac{32}{5} \frac{G^3}{c^5} M_1 M_2 (M_1 + M_2) A^{-4}$$

Non conservative mass transfer

β - mass loss

α – angular momentum loss

$$\beta = -\frac{\dot{M}_2}{\dot{M}_1} \qquad \frac{dJ}{dM} = \alpha \frac{J}{M}$$

IF α and β are constant:

$$\frac{A}{A_0} = \left(\frac{M_d}{M_{d,0}} \frac{M_a}{M_{a0}} \right)^{-2} \left(\frac{M}{M_0} \right)^{2\alpha+1}$$

Angular momentum loss from one star

$$\frac{dJ}{dM_1} = \alpha(1 - \beta) \frac{2\pi A^2}{P} = \alpha(1 - \beta) \sqrt{GMA} = \alpha(1 - \beta) \frac{J}{\mu}$$

$$\frac{A}{A_0} = \frac{M}{M_0} \left(\frac{M_1}{M_{1,0}} \right)^{2\alpha(1-\beta)-2} \left(\frac{M_2}{M_{2,0}} \right)^{-2\alpha(1-\beta)/\beta-2}$$

Mass loss through L2

$$\frac{P}{P_0} = \frac{M}{M_0} \left(\frac{M_{1,0}}{M_1} \right)^{-3[1-\eta^{1/2}(1-\beta)]} \left(\frac{M_{2,0}}{M_2} \right)^{3[1-\eta^{1/2}(1-\beta)/\beta]}$$

when $\beta=0$

$$\frac{P}{P_0} = \frac{M}{M_0} \left(\frac{M_{1,0}}{M_1} \right)^{3[1-\eta^{1/2}]} \exp \left(3\eta^{1/2} \frac{\Delta M_1}{M_2} \right)$$

gdzie

$$\eta = \frac{A_r}{A}$$

$$\beta = -\frac{\dot{M}_2}{\dot{M}_1}$$

Common envelopes

Unstable mass transfer

Acceptor falls in to the donor's envelope

Accretion, ejection of the envelope, coalescence, short timescale

Phenomenological description:

Webbink (1984)

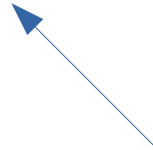
Paczynski, Ziółkowski (1967) , and Nelemans i Tout (2005)

Common envelope

$$\alpha_{CE} (E_{fin}^{orb} - E_{ini}^{orb}) = \lambda^{-1} E_{bind}$$



Efficiency of common
envelope



Envelope structure

$$\alpha_{CE} \left(-\frac{GM_{1f}M_2}{2A_f} + \frac{GM_{1i}M_2}{2A_i} \right) = -\frac{GM_{1i}M_1^{env}}{\lambda A_i r_L}$$

or

$$\frac{A_f}{A_i} = \left(2 \frac{M_1^{env} M_{1f}}{\alpha_{CE} \lambda r_L(q) M_{1i} M_2} + \frac{M_{1i}}{M_{1f}} \right)^{-1}$$

Common envelope

- Possible outcome:
 - Merger
 - Tight binary
- What does it take to succeed?
- What are the unknowns
 - Envelope structure
 - Energy Injection mechanism
 - Timescale
 - Influence on the acceptor

Common envelope – alternative treatment

$$J_f - J_i = -\gamma J_i \frac{\Delta M}{M_{tot}}$$

Efficiency of angular momentum
ejection

$$\frac{P_f}{P_i} = \left(\frac{M_{1i} M_{2i}}{M_{1f} M_{2f}} \right)^3 \frac{M_{1f} + M_{2f}}{M_{1i} + M_{2i}} \left(1 - \gamma \frac{\Delta M}{M_{1i} + M_{2i}} \right)^3$$

The influence of the mass transfer on the stars

- Rejuvenation
- Accretion - brightness
- Rotation
- Chemical composition
- Radii

Stellar coalescence

- Darwin instability
- Low mass ratios
- Common envelopes
- Gravitational waves

Darwin instability

- Tidal forces,
- Corotation
- Angular momentum balance

$$J = I\omega_{rot} + \mu \frac{(GM)^{2/3}}{\omega_{orb}^{1/3}}$$

Darwin instability

- Impossibility to achieve equilibrium
- Change of rotation
- Attempting corotation

$$\frac{d\omega_{rot}}{d\omega_{orb}} = \frac{1}{3} \frac{J_{orb}}{J_{rot}}$$

Supernovae

- Rapid mass loss
- Interaction with companion
- Asymmetries – kicks
-

Orbit change

$$M' = FM$$

$$\frac{\dot{\mathbf{d}}^2}{2} - \frac{GM}{d} = -\frac{GM}{2a}, \quad \frac{\dot{\mathbf{d}}^2}{2} - \frac{GM'}{d} = -\frac{GM'}{2a'}$$

$$\left\langle \frac{1}{a'} \right\rangle = \frac{2 - M/M'}{a} = \frac{1}{a} \left(2 - \frac{1}{F} \right).$$

Ellipticity

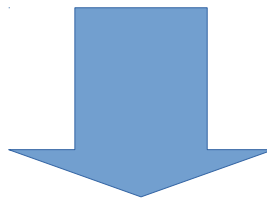
$$GMa(1 - e^2) = |\mathbf{d} \times \dot{\mathbf{d}}|^2 = GM'a'(1 - e'^2).$$

$$\left\langle \frac{a}{a'} \right\rangle = 2 - \frac{1}{F}; \quad \frac{\langle e'^2 \rangle - e^2}{1 - e^2} = \left(\frac{1}{F} - 1 \right)^2$$

Supernovae kicks

$$\frac{1}{2}|\dot{\mathbf{d}} + \mathbf{u}|^2 - \frac{GM'}{d} = -\frac{GM'}{2a'},$$

$$|\mathbf{d} \times (\dot{\mathbf{d}} + \mathbf{u})|^2 = GM'a'(1 - e'^2).$$



$$|\mathbf{u}| \equiv K\sqrt{\frac{GM}{a}}$$

$$\left\langle \frac{a}{a'} \right\rangle = 2 - \frac{1}{F}(1 + K^2),$$

$$\frac{\langle e'^2 \rangle - e^2}{1 - e^2} = \left(\frac{1}{F} - 1 \right)^2 + \frac{K^2}{3F(1 - e^2)} \left[\frac{9 - 8e^2}{F} - 2(2 + e^2) \right] + \frac{K^4}{3F^2} \frac{2 + 3e^2}{1 - e^2}$$

Three types of systems

- Contact
- Filling Roche lobe
- Separate

How does the mass transfer proceed

- Filling Roche lobe
- Change of orbit
- Change of stellar structure
- Both factors influence the fate of the system

Roche lobe change

- Roche lobe radius derivative:

$$R'_L = \frac{d \log R_L}{d \log M_1} \approx 2.13q - 1.67$$

- Works well for $0 < q < 50$

Influence on the donor

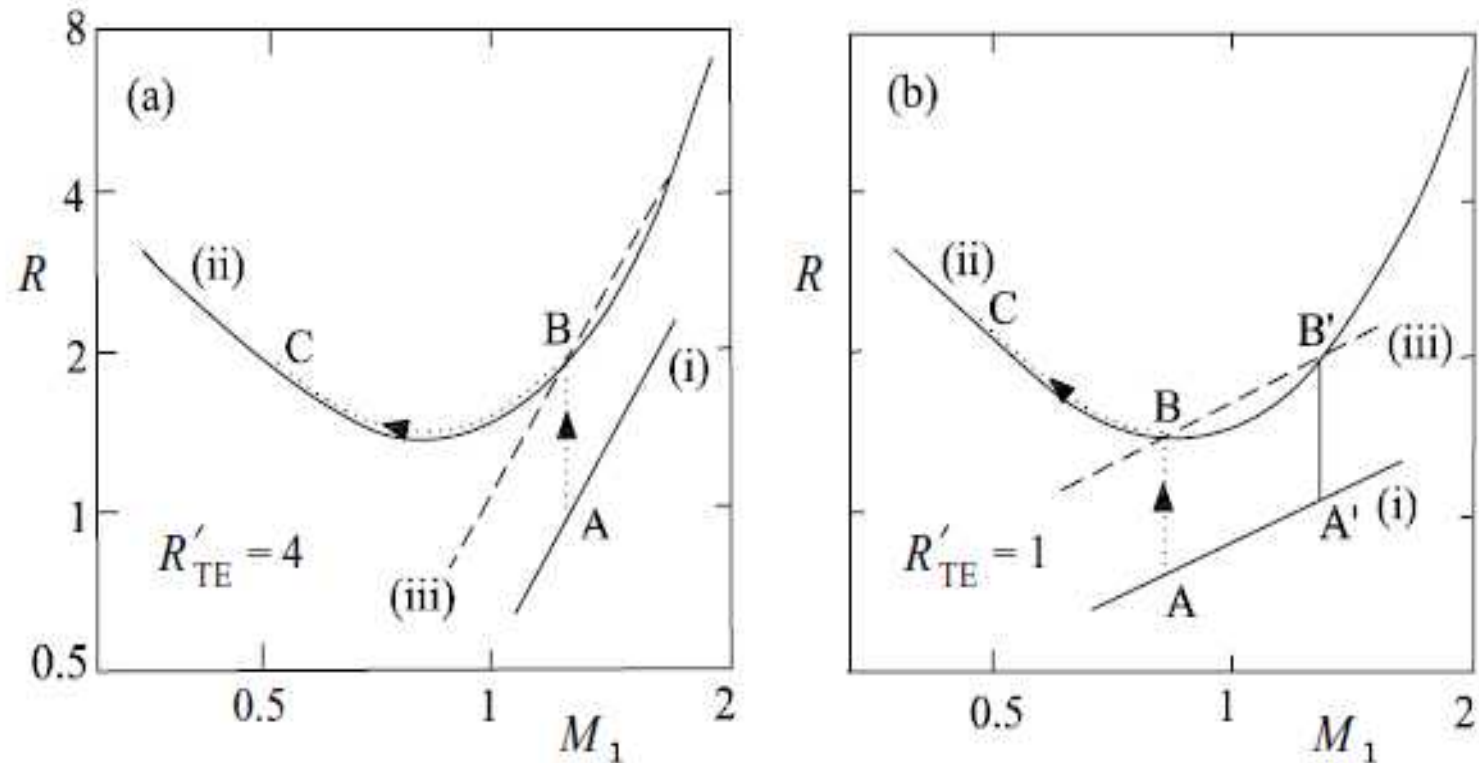


Figure 3.4 Schematic behaviour of Roche-lobe radius and stellar radius as functions of primary mass during evolution governed by the simplistic relation (3.52). Units are arbitrary, except that the total mass is 2 units. The curves are (i) the ZAMS radius, (ii) the Roche-lobe radius, (iii) the radius at time $t = t_{NE} \log 2$. The star starts on curve (i), at point A or A', and evolves vertically until it reaches curve (ii) at B or B'. From B in either panel, it can proceed to evolve along curve (ii) to C, losing mass while still evolving on a nuclear timescale. In (b) it cannot do this from point B', since curve (ii) is steeper than curve (iii) there.

Donor structure

- Mass radius relation

$$\log R = \log R_0 + R'_{TE} \log \frac{M_1}{M_0} + \frac{t}{t_{NE}}$$

- Evolution on the nuclear timescale
- Mass transfer:

$$\frac{d \log M}{t} = \frac{1}{t_{NE}(R'_{TE} - R'_L)}$$

More realistic case

- Thermal timescale transfer
- Star out of equilibrium
- Additional source of energy
- Convective envelope expand, radiative envelopes shrink with mass loss
- On the main sequence – $M < 0.75 M_{\text{sun}}$ – convective envelope

$$\log R = \log R_0 + R'_{TE} \log \frac{M_1}{M_0} + \frac{t}{t_{NE}} + R'_{TD} t_{KH} \frac{d \log M_1}{dt}$$

What does the acceptor do

- Reverse as donor :-) - radiative expands, convective shrinks
- But: different temperature, composition + kinetic energy
- Different timescales than for the donor
- Acceptor may also fill it Roche lobe

Donor and acceptor - evolution

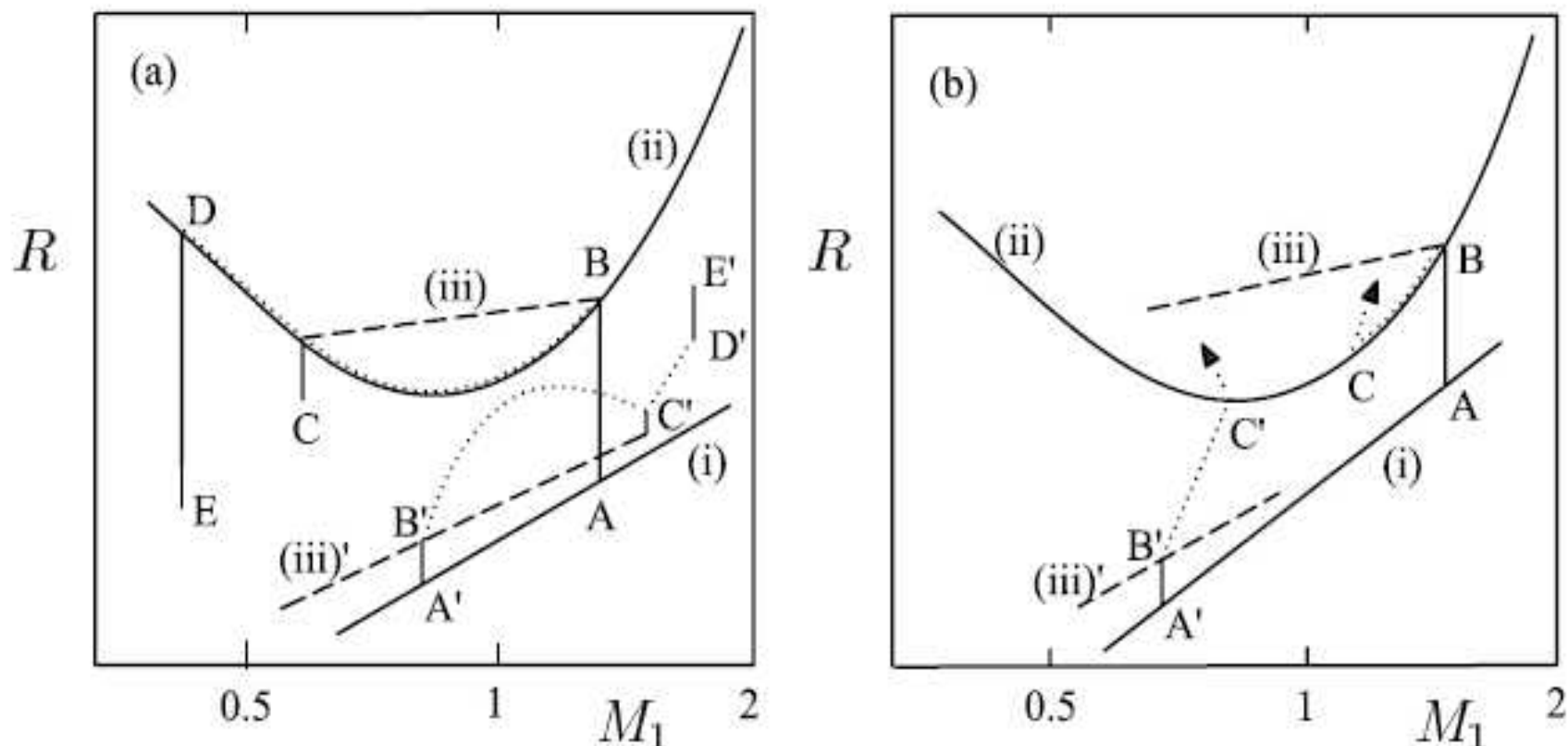


Figure 3.7 Schematic behaviour of radius and mass for both loser and gainer, in situations (a) where the gainer does not expand to fill its own lobe, and (b) where it does. Curve (i) – ZAMS; curve (ii) – Roche-lobe radius; curve (iii) – thermal-equilibrium radius. Primed letters indicated *2's position corresponding to the unprimed letter for *1. In (a), after Pennington (1986), the transition from mode 2 to mode 1 was interrupted at point C by a brief detached phase (see text). In (b), after Robertson and Eggleton (1977), evolution beyond contact was followed using a prescription like Eqs (3.85) and (3.86).

Types of mass transfer

- Timescales: nuclear, thermal, hydrodynamical
- Stellar evolution
- Cases A,B,C
- Characteristic parameters: R'_{TE} , R'_{TD}
- Comparison with R'_L determines the mass transfer type as a function of q at the moment of Roche lobe filling

Types of mass transfers

$$R'_{TE} = R'_L(q_{cr}) = 2.13q_{cr} - 1.67$$

- First - nuclear

$$q < q_{cr}(R'_{TE}, R'_{TD})$$

- Second - thermal

$$q_{cr}(R'_{TE}) < q < q_{cr}(R'_{TD})$$

- Third – hydrodynamic

$$q_{cr}(R'_{TD}) < q$$

What else can cause mass transfer

- Mass loss
- Magnetic braking – angular momentum loss
- Gravitational waves
- Many body interactions

Typical scenario

- Initially type 2
- Change of q and stability criterion
- Stabilization, mass transfer becomes type 1
- Typically mass ratio reversal
- $R'_{TE}=0.5$ for low masses at ZAMS, for higher masses R'_{TD} is between 0 and -0.33 \rightarrow more than mass ratio reversal

The zoo of binaries



Symbiotic stars

- Giant + compact object (WD, NS, BH?)
- Wide orbits
- Slow mass transfer
- Old disk population
-

Binaries with compact objects

- Accreting: HMXB, LMXB, Be
- Binaries with pulsars: NS-WD, NS-NS
- Binary pulsars
- Binary black holes

Evolution of compact object binaries

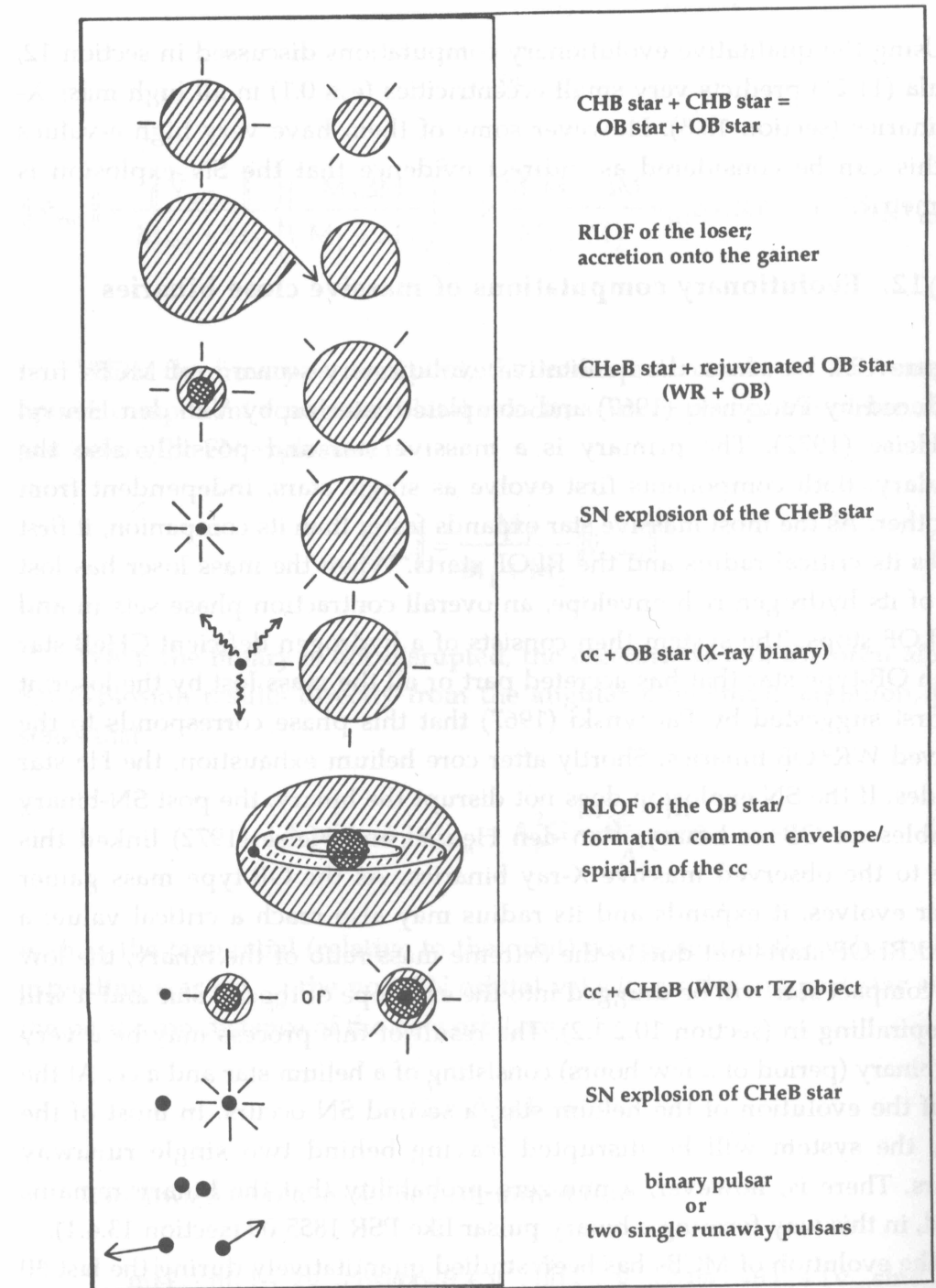


Figure 12.1: The qualitative MCB scenario as it was introduced by Paczynski (1967) and completed by Van den Heuvel and Heise (1972).

Formation of a BH-BH binary

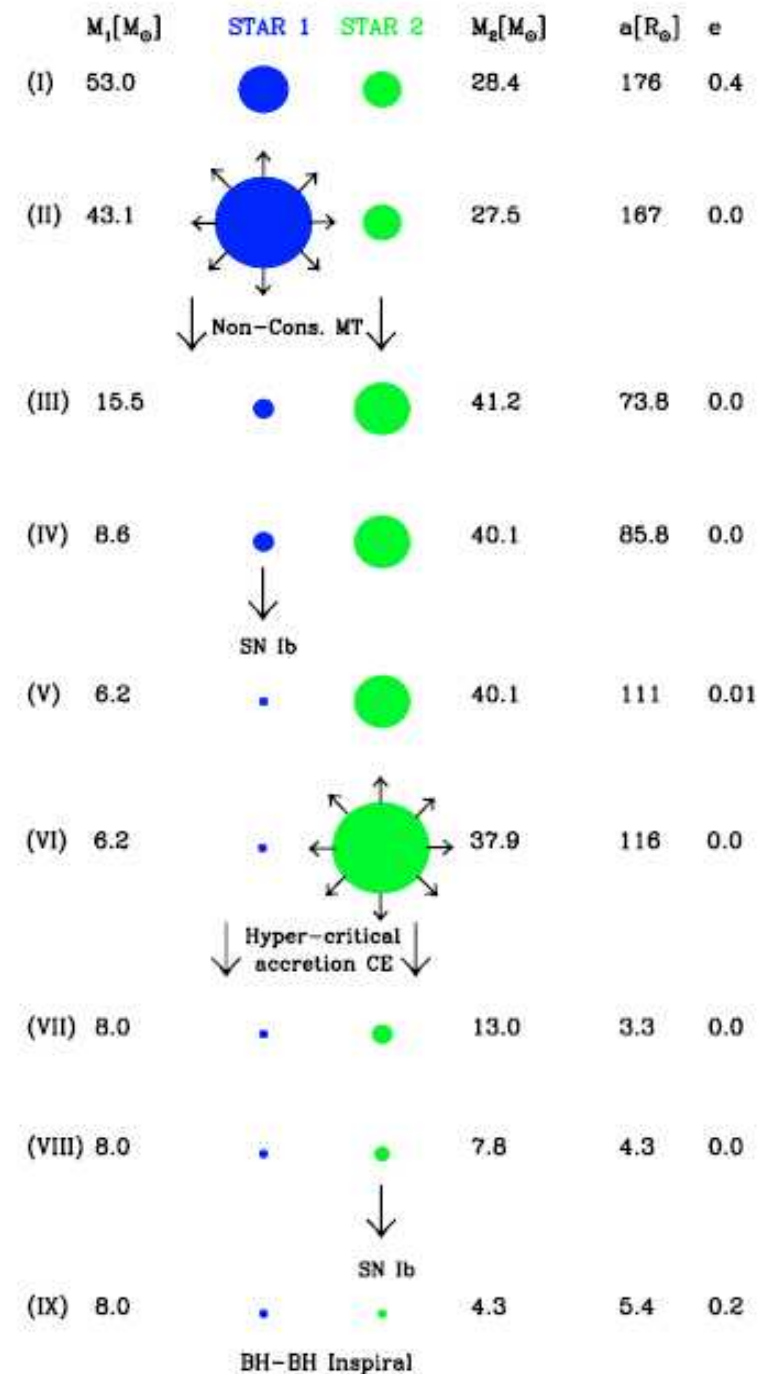


Fig. 1. An example evolutionary scenario leading to formation of a double black hole binary. For details see the text.

Double neutron star binaries:
Additional phase of common
envelope with He star possible

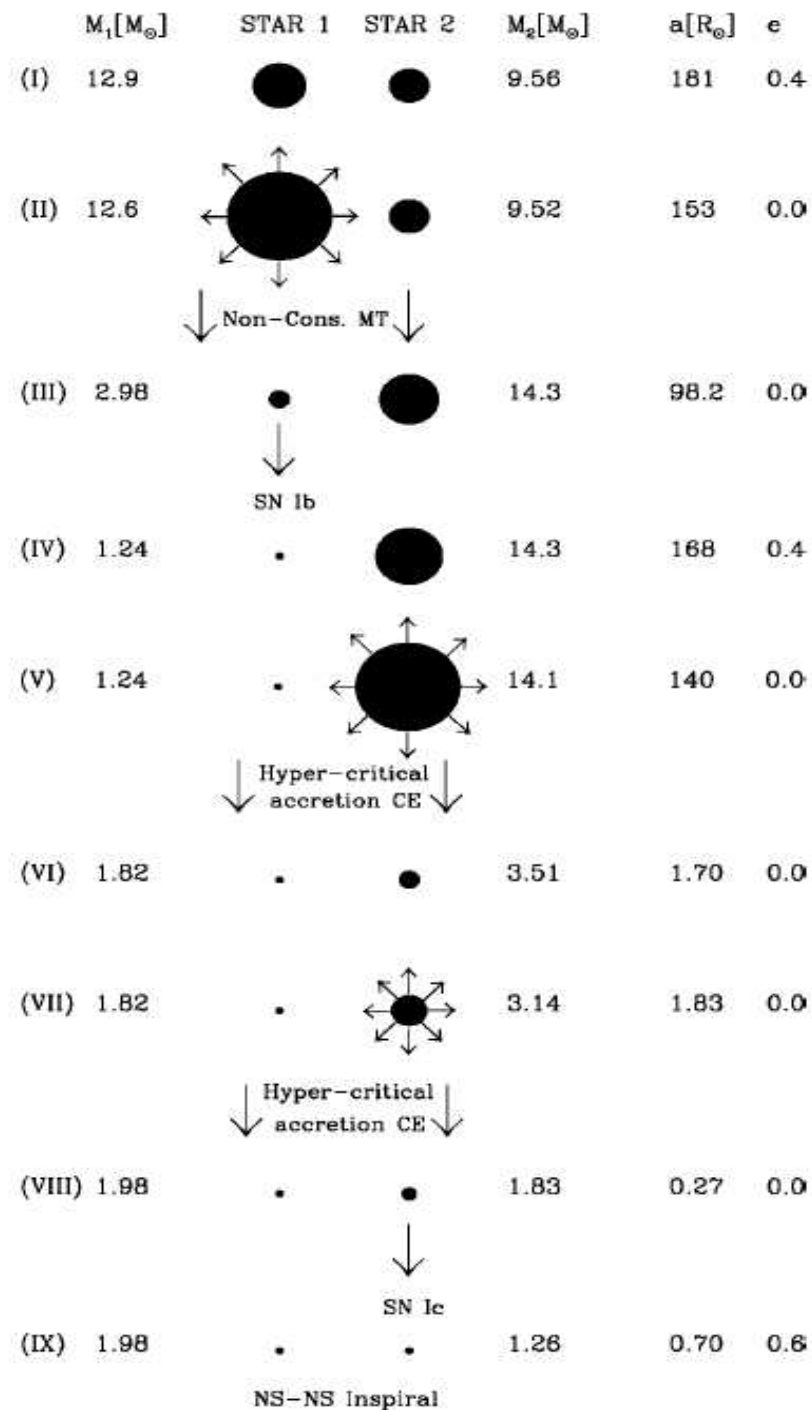


FIG. 1.—Stages of the dominating NS-NS formation path; after 23 Myr of evolution and two SNe, a tight NS-NS binary with a merger time of about 0.7 Myr is formed (details are given in § 3.1).

End products

- Single stars: “mergers”, solitary Bhs, neutron stars
- Compact objects – solitary, binarye (NSNS, BHNS, BHBH)
- Thorne-Żytkow objects
- ...

Binaries with compact objects

- X-ray binaries
 - BH
 - NS
- Binary pulsars (radio, GW)
- Pulsar + star, VHE sources
- Gamma ray bursts?

Where do binary black holes come from?

Tomek Bulik

University of Warsaw

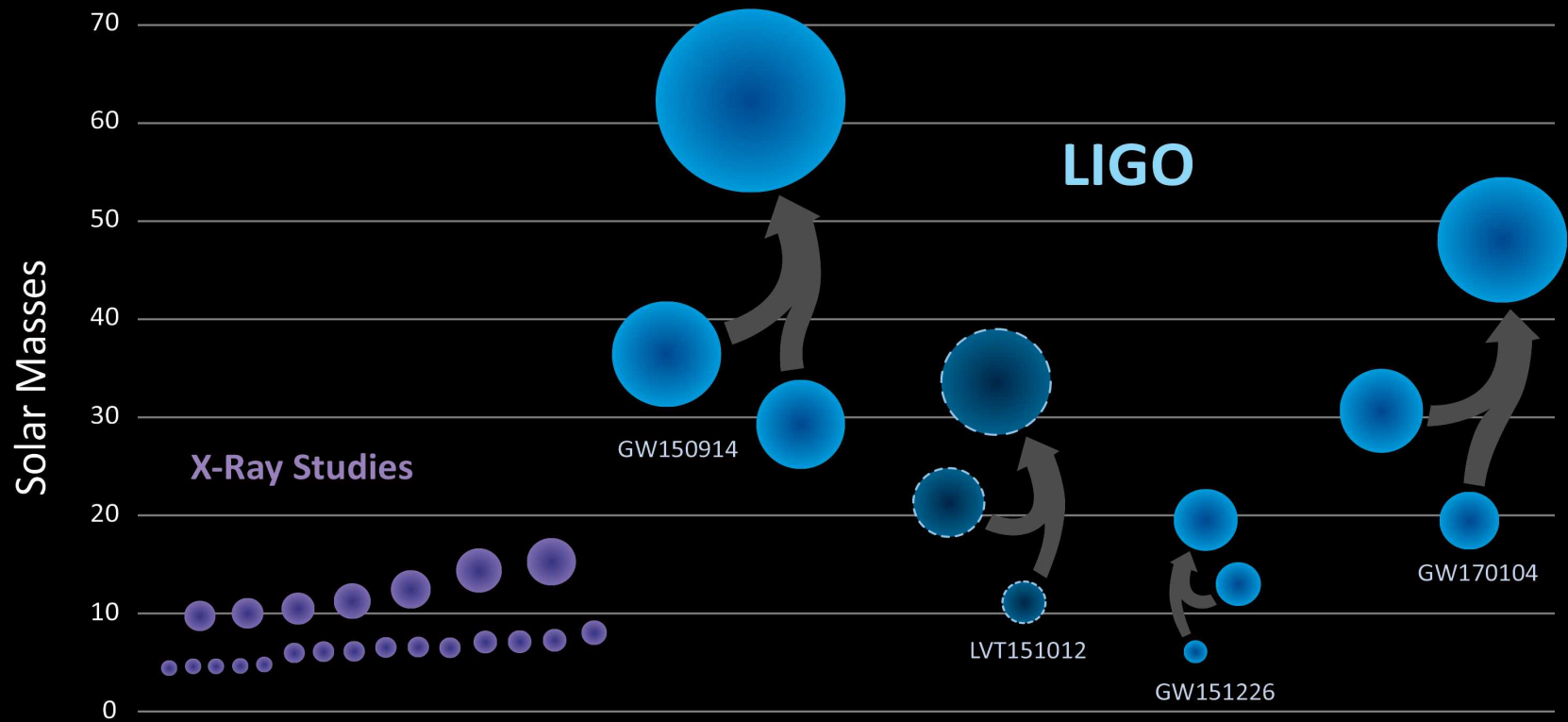
Observations

- Three objects (or 2½)

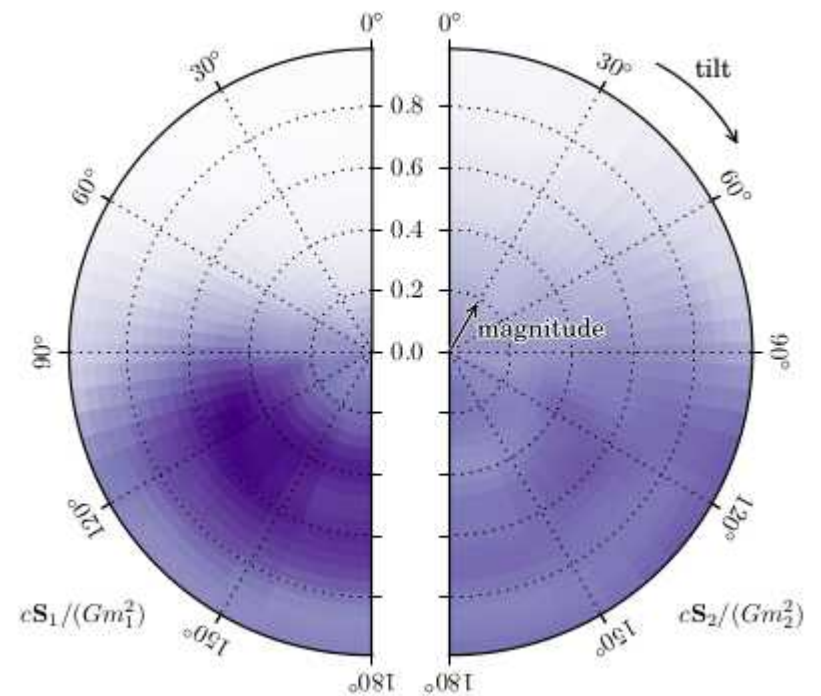
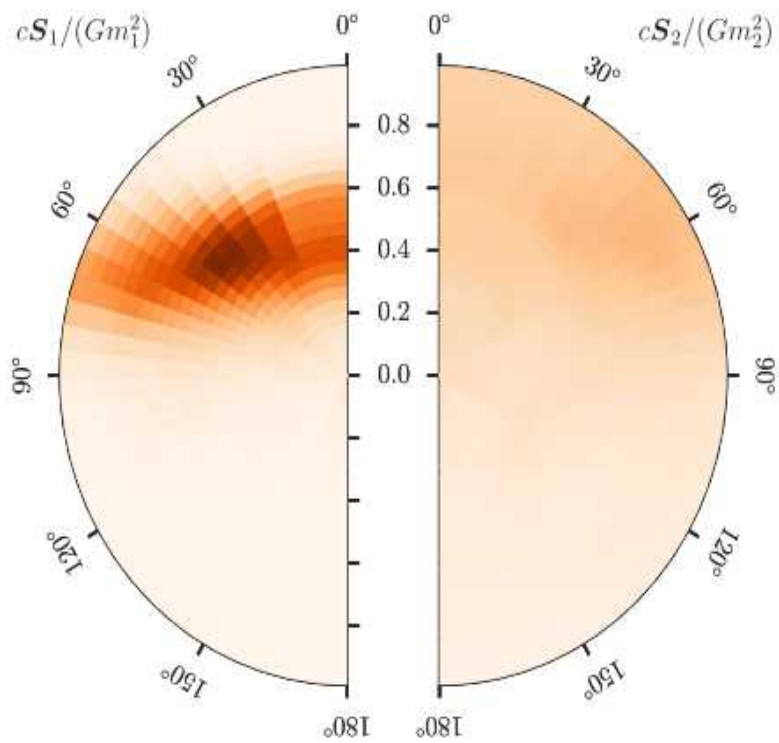
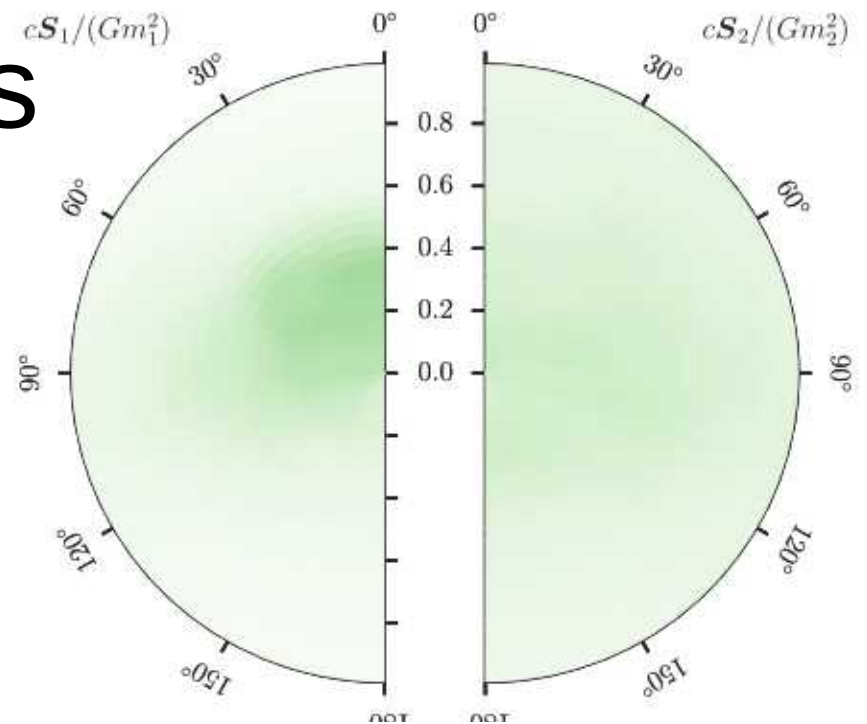
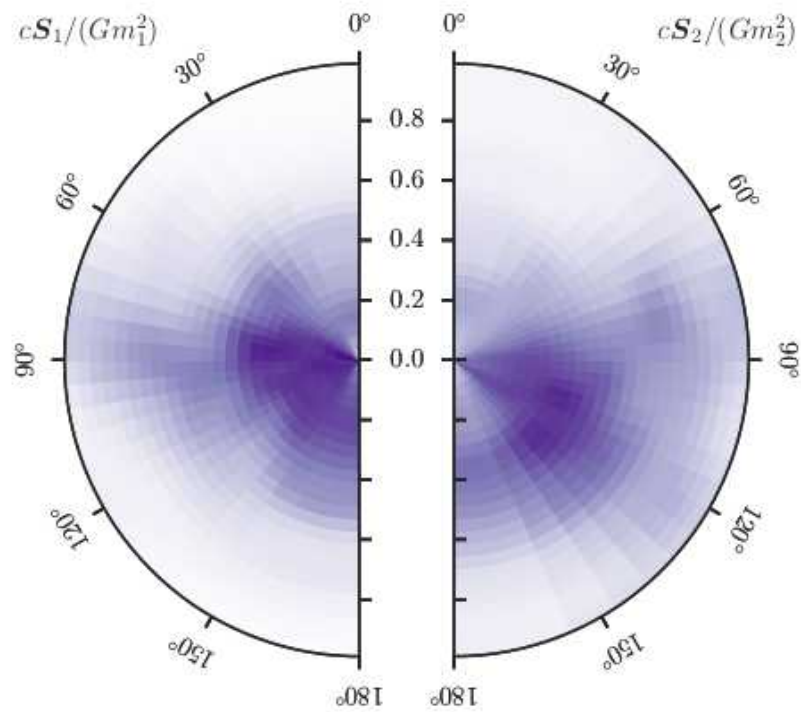
Event	GW150914	GW151226	LVT151012	GW 170104
Signal-to-noise ratio				...
ρ	23.7	13.0	9.7	..
False alarm rate				...
FAR/yr ⁻¹	$< 6.0 \times 10^{-7}$	$< 6.0 \times 10^{-7}$	0.37	...
p-value	7.5×10^{-8}	7.5×10^{-8}	0.045	
Significance	$> 5.3 \sigma$	$> 5.3 \sigma$	1.7σ
Primary mass				
$m_1^{\text{source}}/M_\odot$	$36.2^{+5.2}_{-3.8}$	$14.2^{+8.3}_{-3.7}$	23^{+18}_{-6}	31
Secondary mass				
$m_2^{\text{source}}/M_\odot$	$29.1^{+3.7}_{-4.4}$	$7.5^{+2.3}_{-2.3}$	13^{+4}_{-5}	20

Masses

Black Holes of Known Mass



Spins



BBH formation challenges

- Masses
 - How to obtain such masses in stellar evolution?
- Separation
 - How to bring the BHs together so that they merge in a time shorter than the Hubble time?
- Number
 - How to make them in large numbers so that we explain the detection rate?

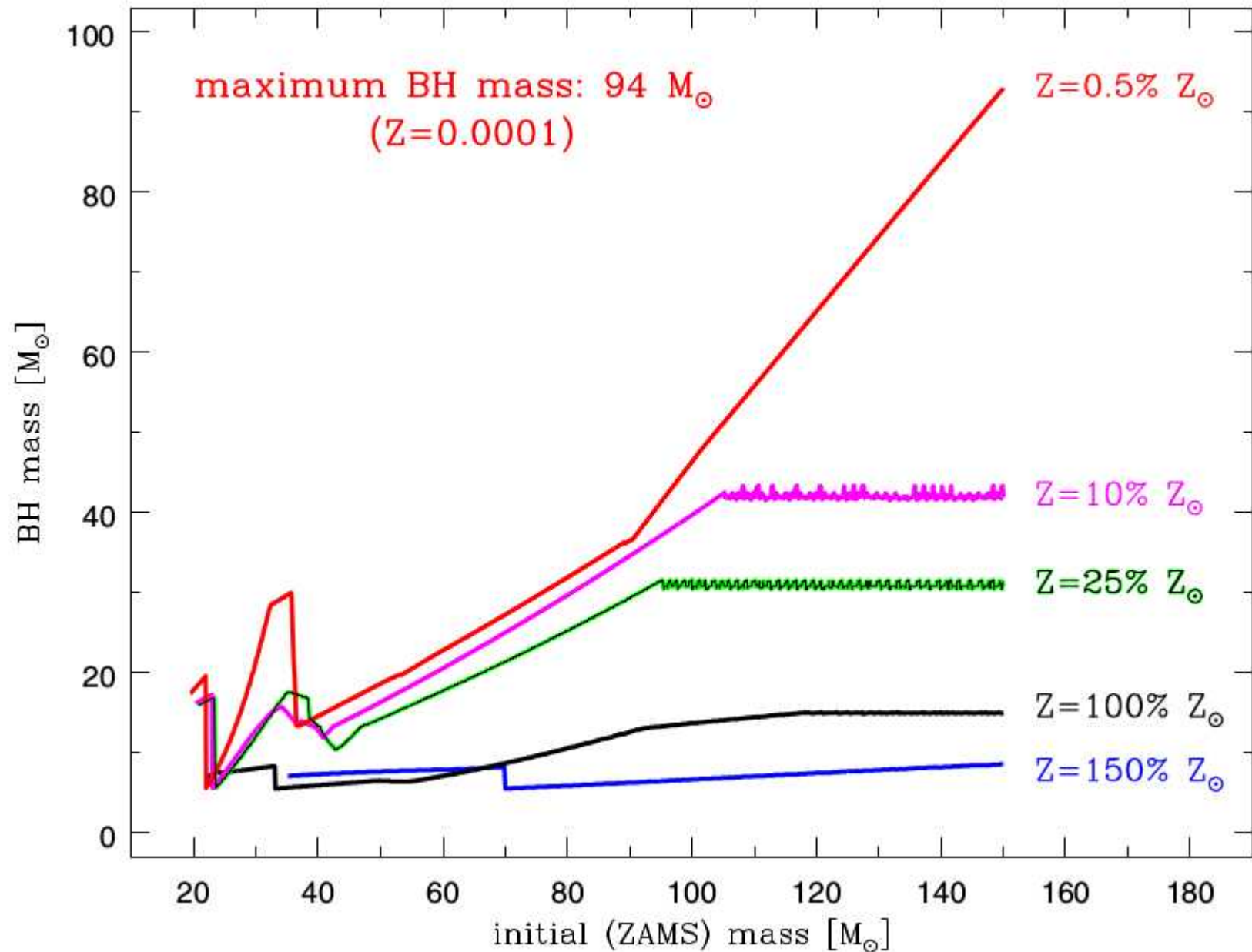
Three (2.5) principal models

- Standard Binary evolution
- Evolution in the Globular clusters
- Chemically homogenous evolution in binaries.

The BHBH merger rate density

- Current estimate 12-213 $\text{Gpc}^{-3}\text{yr}^{-1}$
- The local supernova rate $\sim 10^5\text{yr}^{-1}\text{Gpc}^{-3}$
- The BH formation rate is $\sim 10^4\text{yr}^{-1}\text{Gpc}^{-3}$
- About 1 black hole in a 1000 to a 100 ends up in a merging binary
- It is a lot!

On the maximum mass of BHs



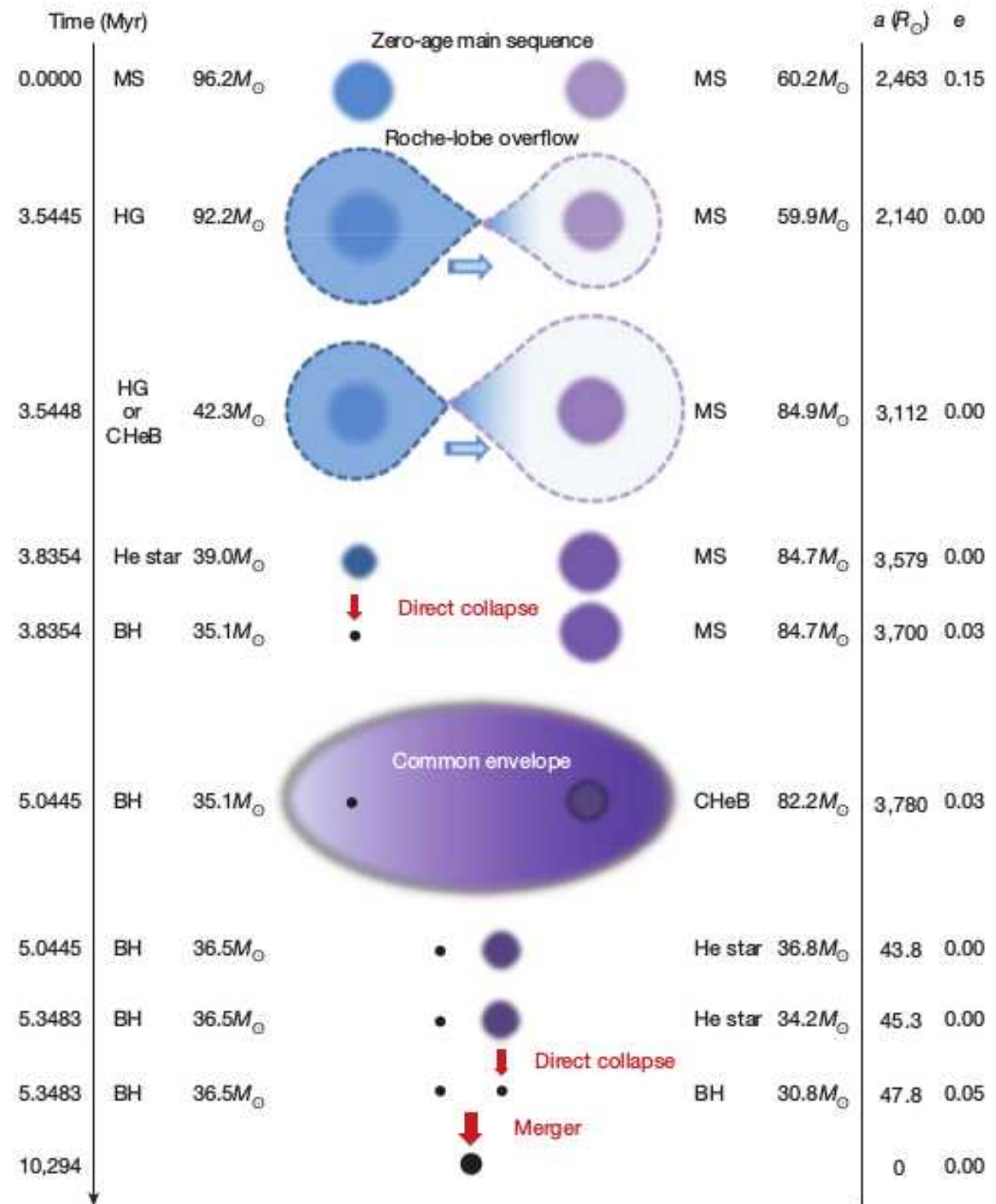
The standard evolution of binaries leading to a BH-BH

- The scenario
- The importance of metallicity

Evolutionary scenario

What brings them together?

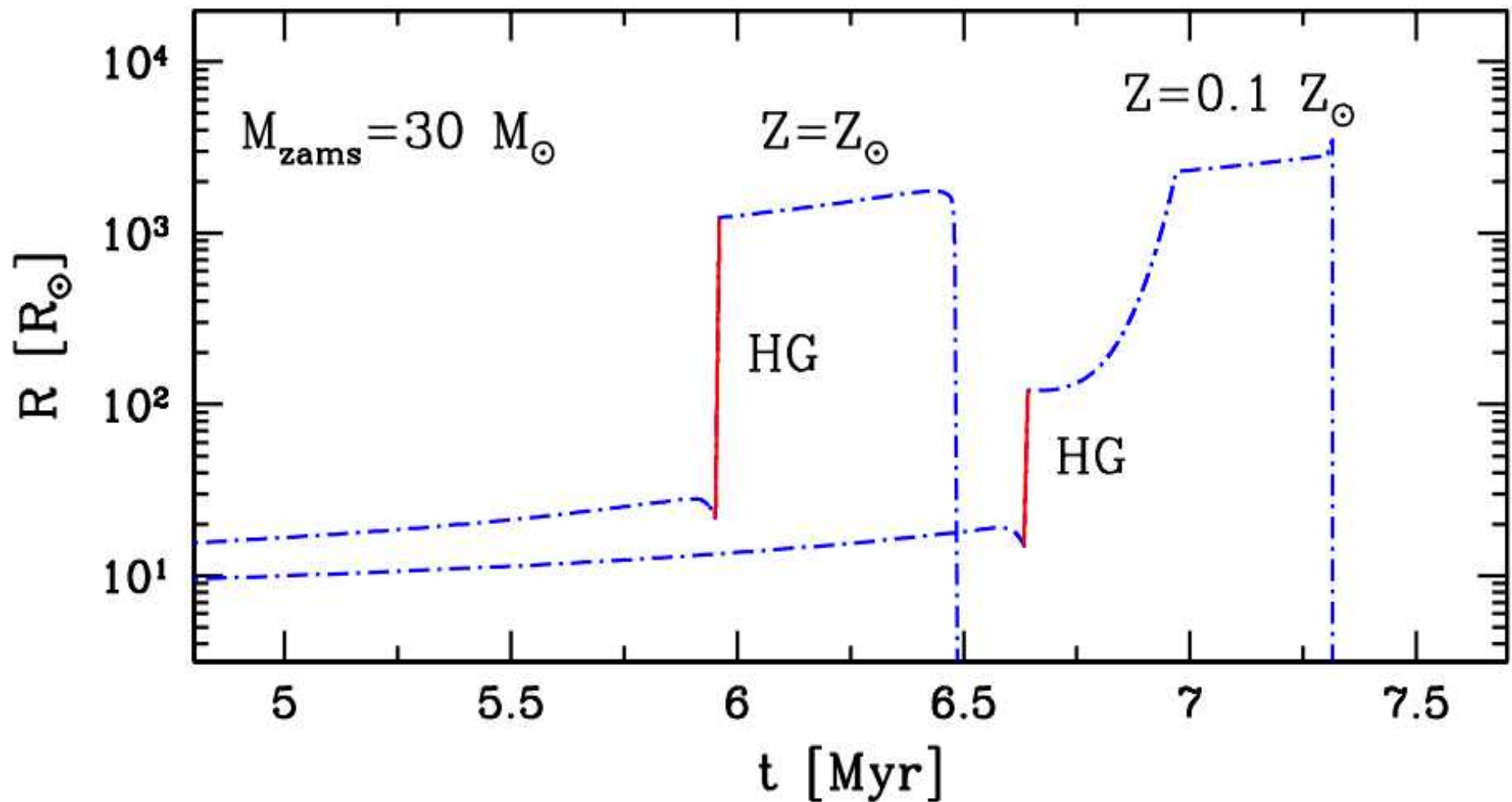
Common envelope:
the bottleneck of BBH formation



How to go through the bottleneck?

- The donor must have clear core-envelope structure
- The CE phase must not result in a merger
- For solar metallicity CE events are likely to result in mergers
- Low metallicity helps:
 - Higher BH masses
 - Lower radii on Hertzsprung gap
 - Higher probability of surviving the common envelope.

Stellar radii



Low metallicity star are typically smaller. Hertzsprung Gap smaller

Population III binaries

- Why stop at low metallicity – let us go extreme!
- Population III
 - High mass stars: probably 10 to a few hundred solar masses
 - Easy formation of massive BHs
 - Amount of mass tightly constrained by reionization
 - Need to form binaries that wait 10-13Gyrs for merger
 - Very few observational constraints in the nature of PopIII stars and binaries.

Chemically homogeneous evolution

- Alternative scenario
- Stars rotate quickly, and are chemically homogeneous throughout the evolution
- Stars do not expand
- Avoid the need for common envelope
- Form binaries a mass ratio close to unity
- Interesting possibility – subclass of binaries

Formation in Globular Cluster

- Dense stellar regions
- Multibody interactions
- Formation of binaries with heavy BHs
- Additional velocities- escapers
- Some – very few quicky merging encounters
- Delay distribution

Properties of a population

- BHBH production efficiency:
 - Number of merging BBH per unit mass
- Delay times
- Mass distribution
 - Intrinsic vs observed: range and redshift effect
- Rate density: local and as a function of redshift

BBH production efficiency

$$X_{BH\,BH} = \frac{N_{BH\,BH}}{M_*}$$

If all BHs end up in merging binaries and with Salpeter IMF

$$X_{BH\,BH}^{max} = 6 \times 10^{-4}$$

Our simulations show:

$$X_{BH\,BH} \approx 10^{-7} \quad \text{for } Z = Z_{\odot}$$

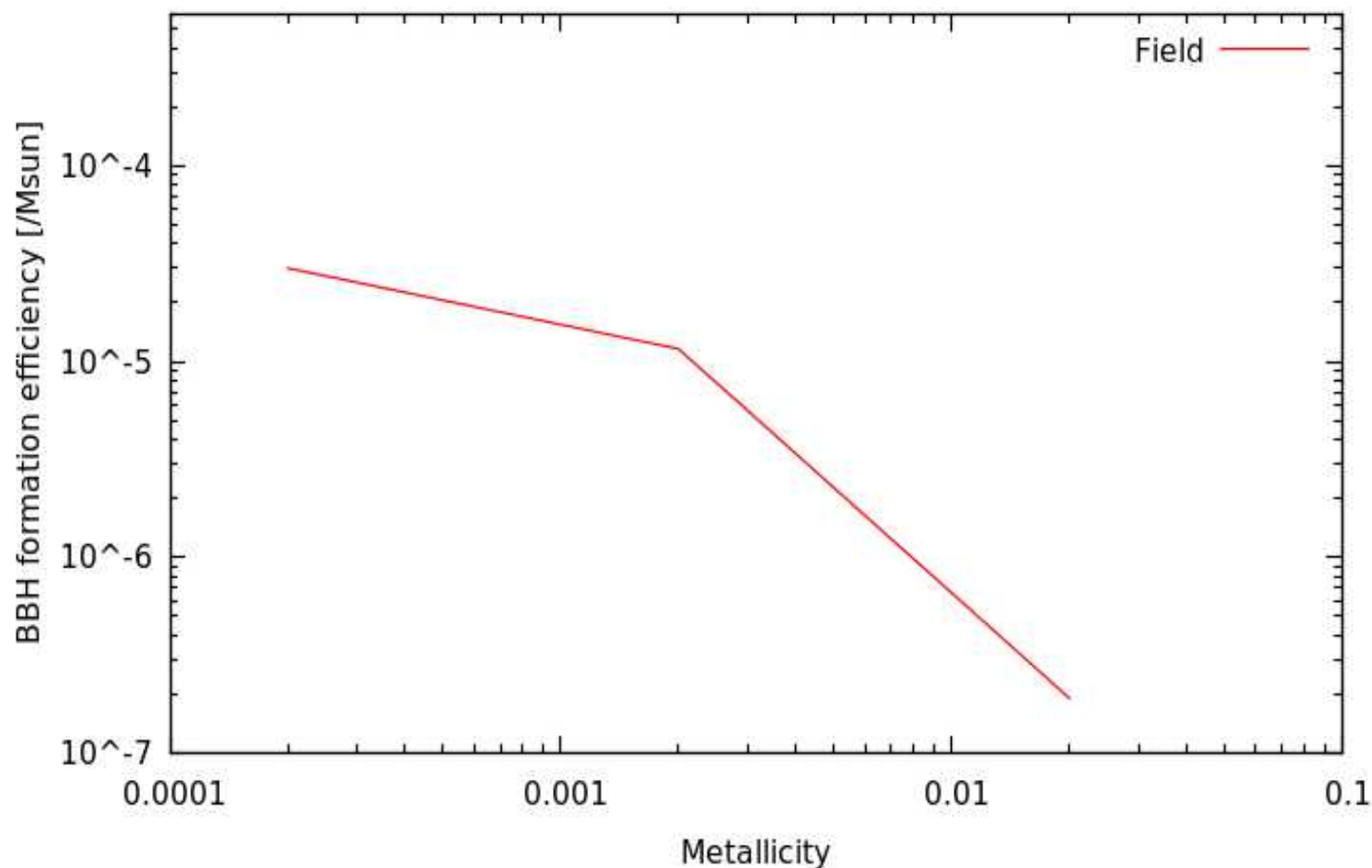
$$X_{BH\,BH} \approx 10^{-5} \quad \text{for } Z = 10\% Z_{\odot}$$

$$X_{BH\,BH} \approx 3 \times 10^{-5} \quad \text{for } Z = 1\% Z_{\odot}$$

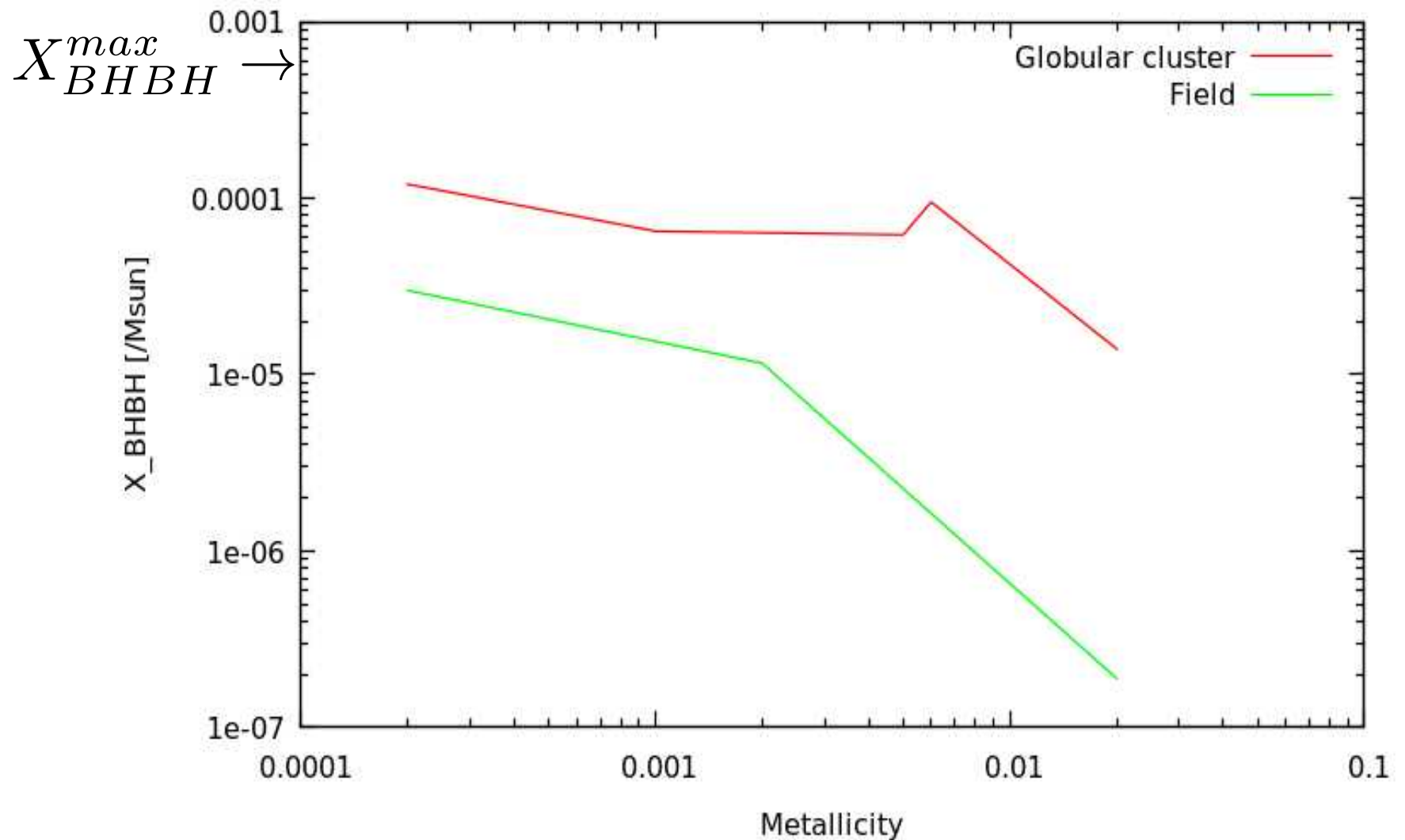
BHBH formation efficiency

$$X_{BHBH} = \frac{N_{BHBH}}{M_*}$$

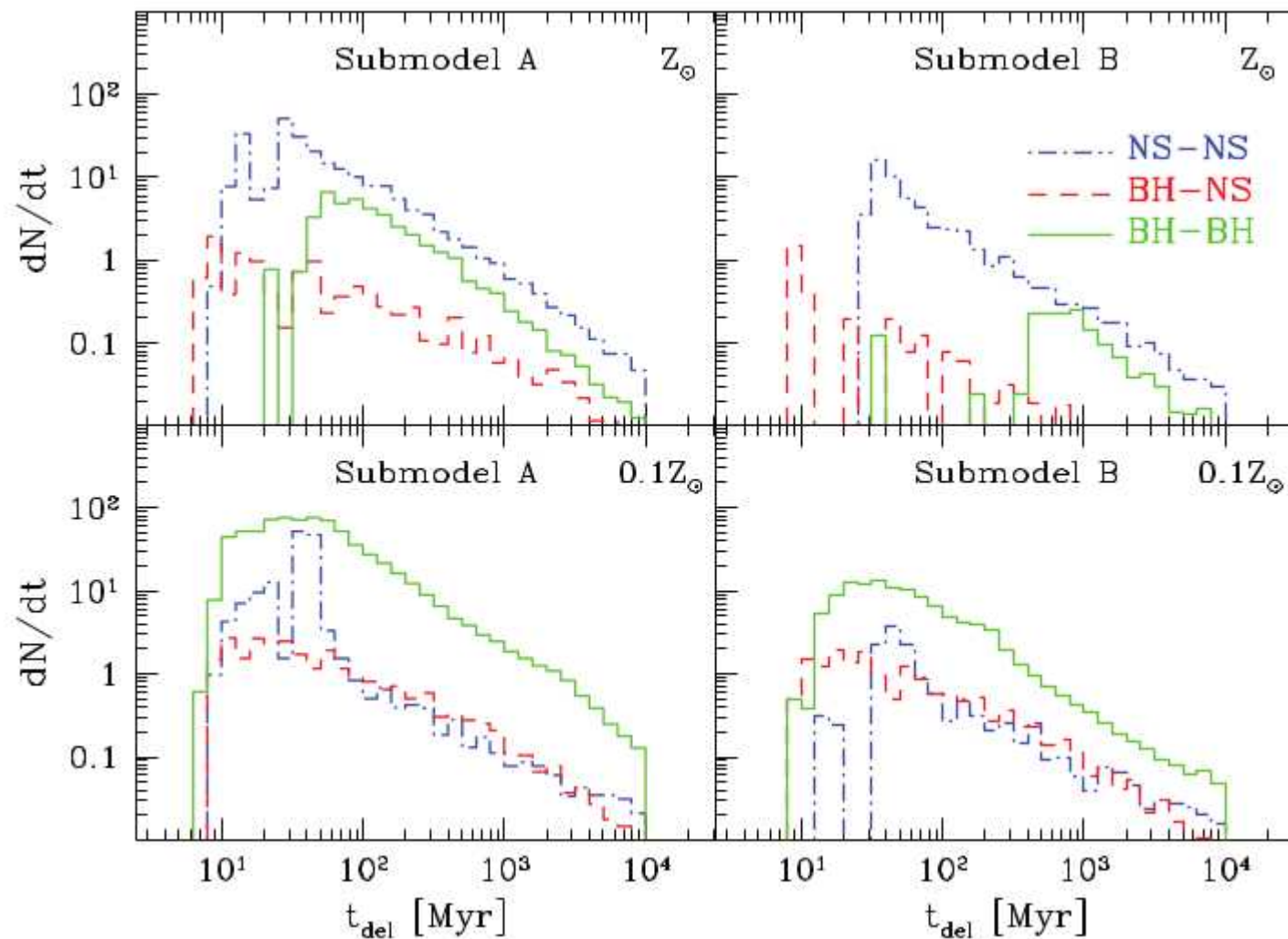
If all BHs end up in merging binaries
and with Salpeter $X_{BHBH}^{max} = 6 \times 10^{-4}$



Globular cluster BHBH formation efficiency

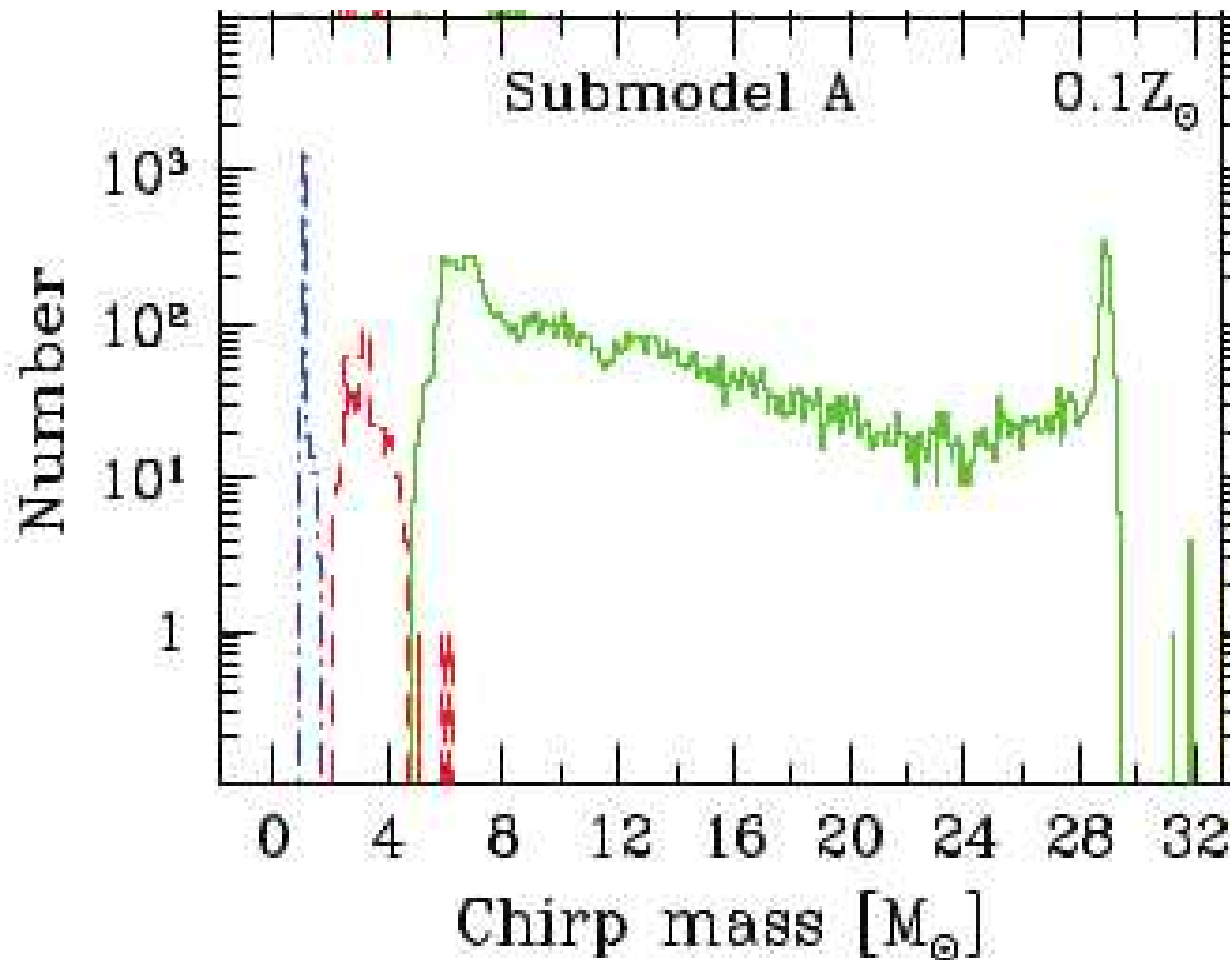


Properties of the population – delay time distribution



$$P_{\text{delay}}(t) \propto t^{-1}$$

Properties of the population – mass distribution

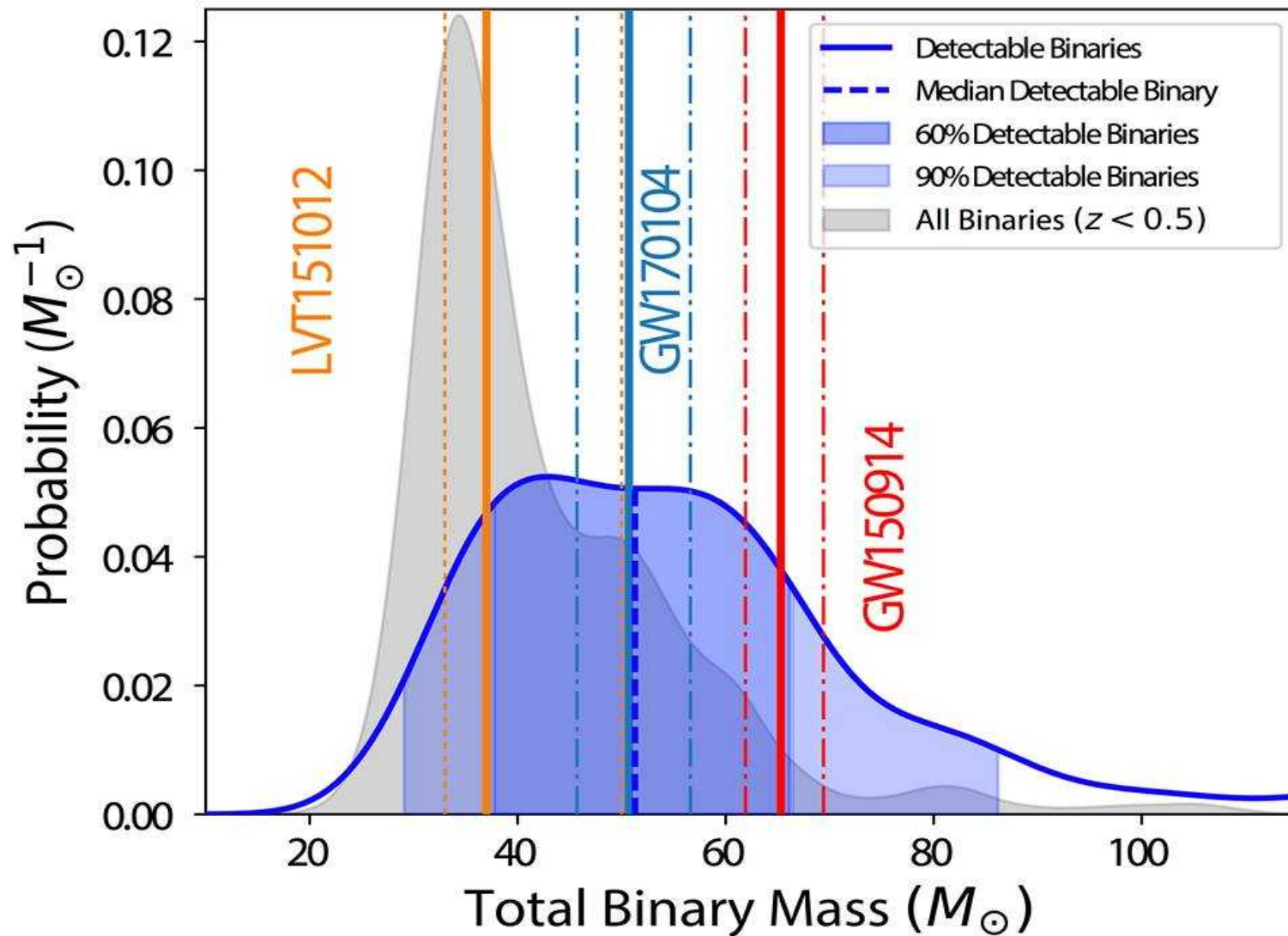


Remember the distinction between intrinsic and observed mass distribution – sensitivity selection effect and redshift

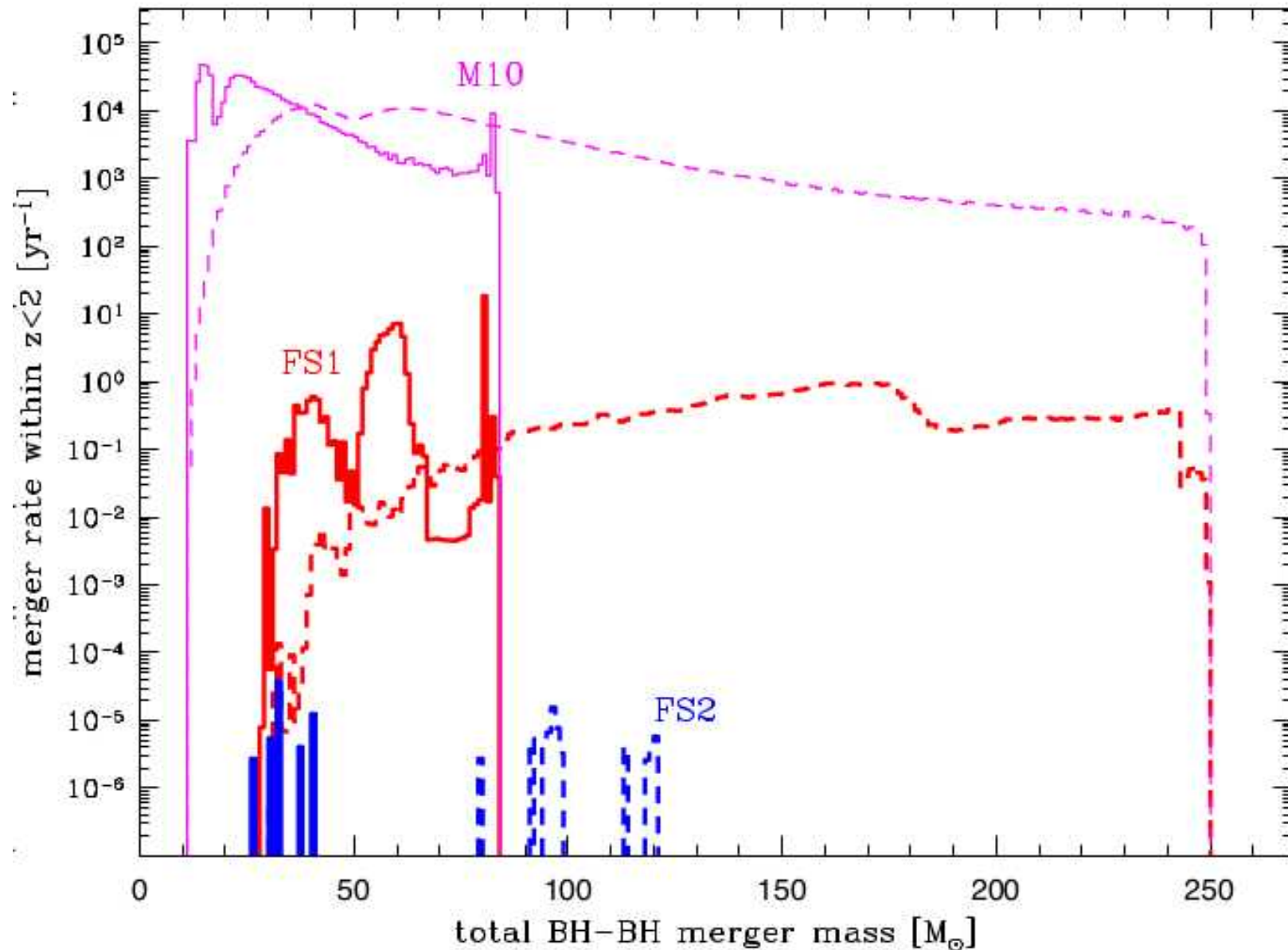
Must take into account lower metallicities, and higher chirp masses

With lower metallicity masses can be greater.

Masses – clusters



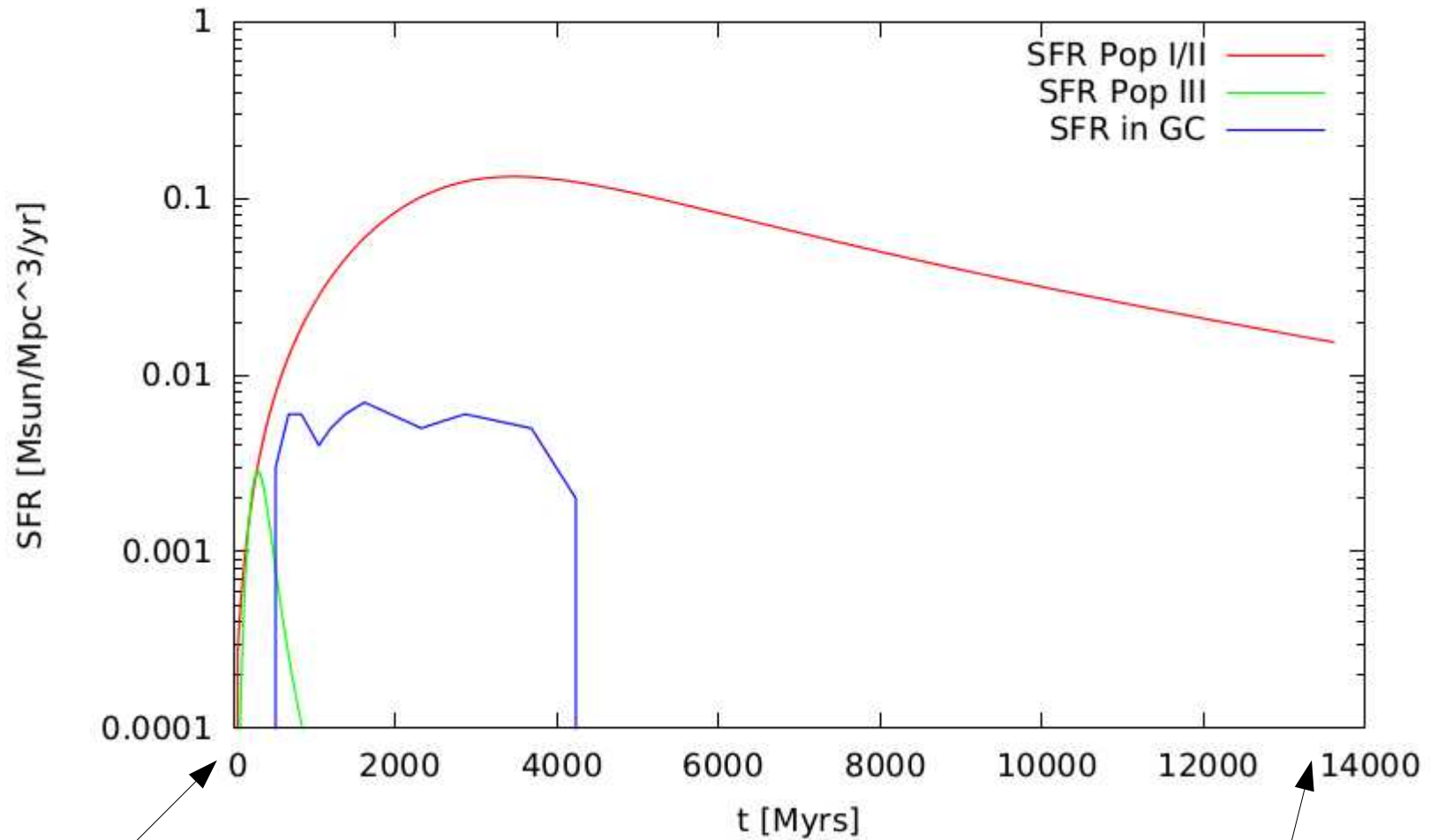
Pop III BHBH - masses



Merger rate density calculation

- Ingredients: $\mathcal{R} = \int dt SFR(t_{now} - t) X_{BH BH} P_{delay}(t)$
 - SFR,
 - BBH production efficiency,
 - delay time distribution,
 - mass distribution
- Two limiting cases:
 - Old population: rate density dominated by the tail of delay distribution
 - Recent population: rate density dominated by the recent star formation
- Rate density should increase with redshift z

SFR



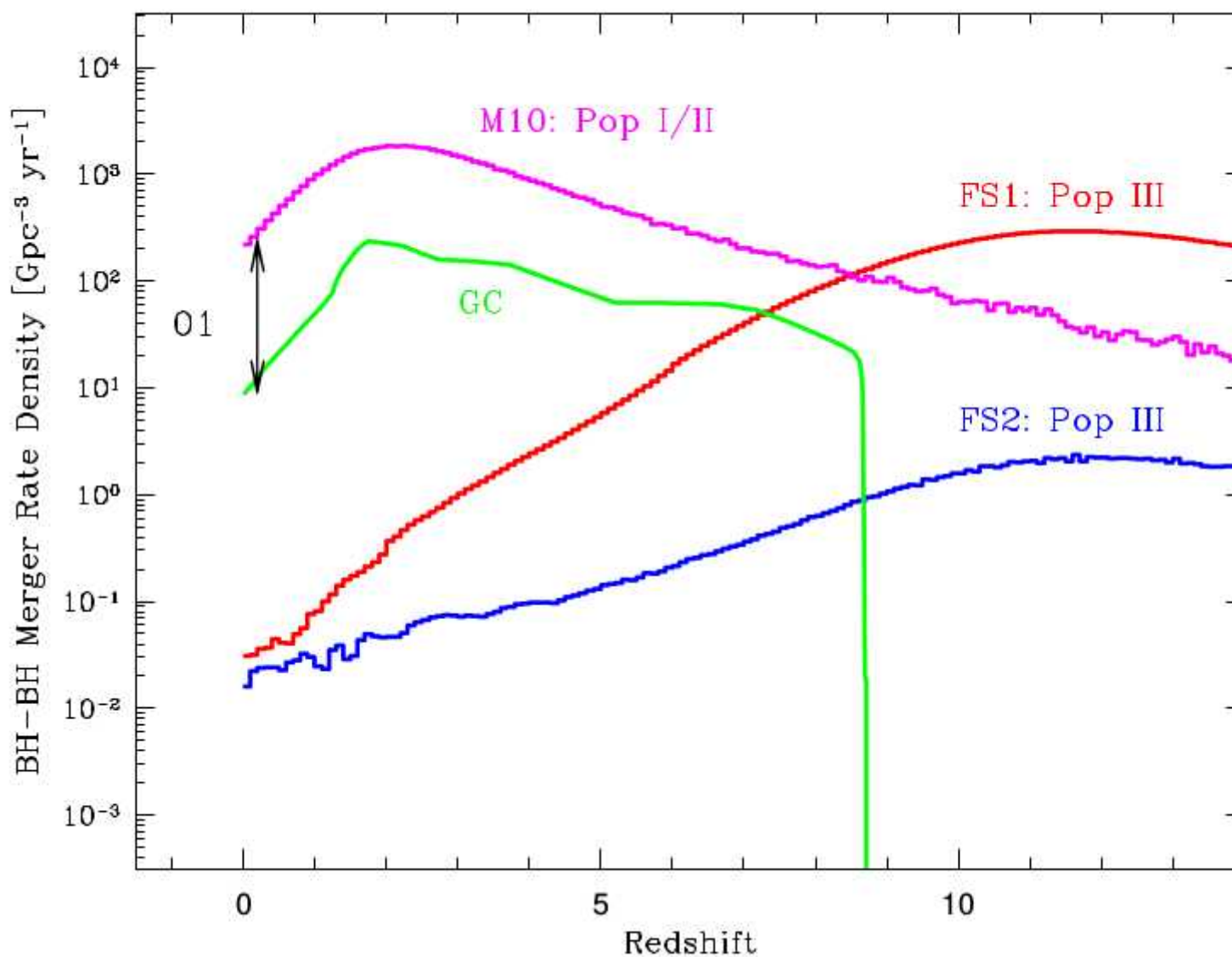
On the merger rate density at $z=0$

- Integrated SFR:
 - Pop III – only $\sim 0.1\%$
 - GC $\sim 1\%$
- Pop III BHBH production efficiency higher because of lack of low mass stars:

$$X_{BHBH}^{PopIII} \approx 6 \times 10^{-4}$$

- We see only the very tail of the delay distribution
- Similar arguments limit the GC rate

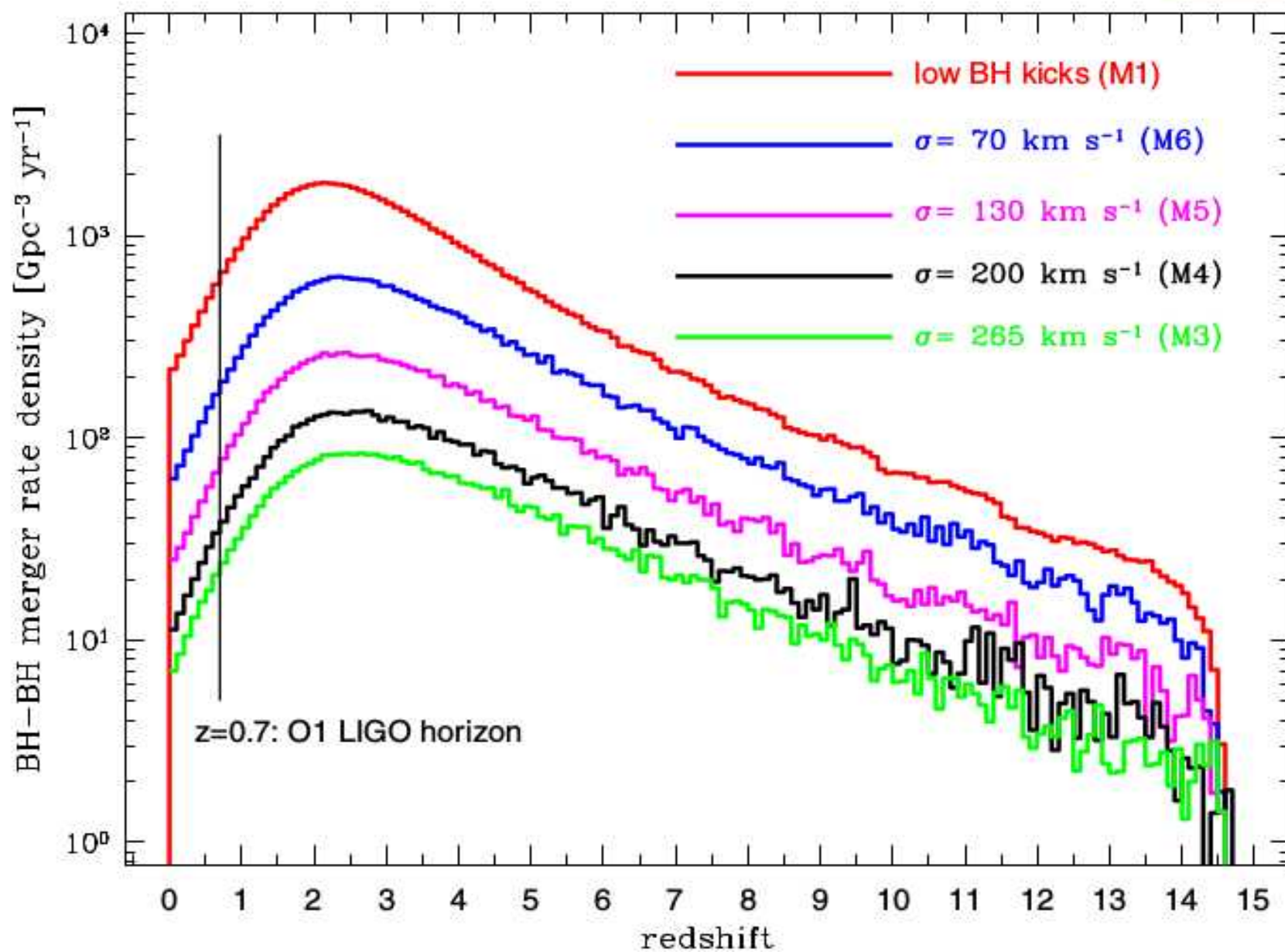
Comparison with other models



Globular cluster vs Pop I/II

- SFR integral – a factor of ~ 0.01
- Formation efficiency difference < 10
- Delays a factor between 0.5 and 0.1
- Summary: GC rate is 0.05 to 0.01 of the field rate

Rate density evolves!



Observational consequences: X-ray binaries

- The peculiar cases of IC10 X-1 and NGX300 X-1
- WR X-ray binaries, ~ 1 day periods
- Are the companions black holes?
 - Ionized wind model
- If so, they fit the picture
- If not – we should look for them!!
- ULXs!

The twin WR binaries

IC10 X-1

- $M_{\text{BH}}=23\text{-}33 \text{ Msun}$
- $M_{\text{WR}}=17\text{-}35 \text{ Msun}$
- $P=35\text{h}$
- Host metallicity=0.3

NGC300 X-1

- $M_{\text{BH}}=14.5\text{-}20 \text{ Msun}$
- $M_{\text{WR}}=15\text{-}26 \text{ Msun}$
- $P=32\text{h}$
- Host metallicity=0.6

Tight binaries with a massive BH accreting from a WR star in a low metallicity region

The case of IC10 X-1

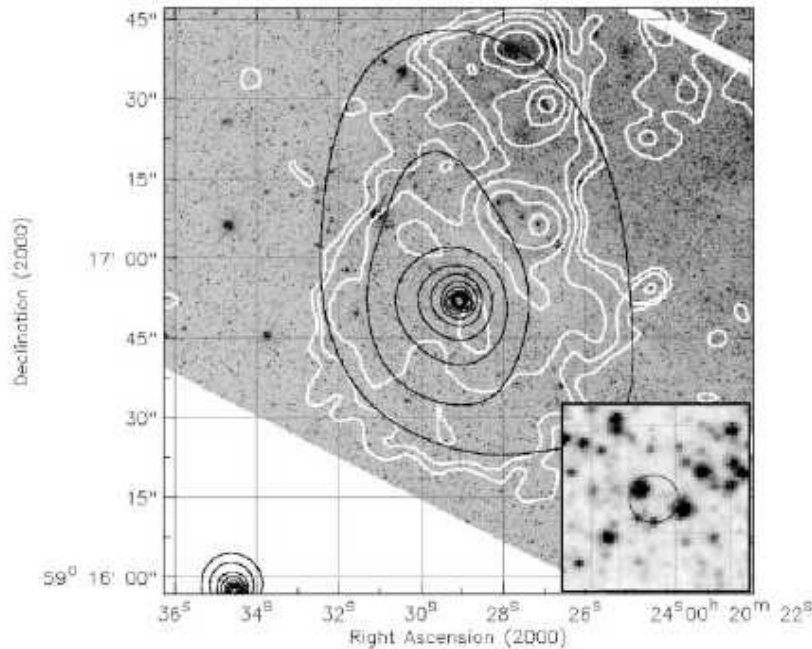


FIG. 1.—X-ray (*dark*) and radio (*light*) contours in the vicinity of X-1 overlaid on the *HST* ACS F814W image. The image shows X-1 in relation to the X-ray and radio emission from the surrounding superbubble. *Inset*: 50 pixel ($\approx 2''.2$) close-up of X-1 indicating the $0''.30$ X-ray error circle (statistical+systematic), relative to the ACS F814W counterparts. X-1 lies $0''.23$ from the confirmed W-R star [MAC92] 17A (slightly above and to the left of the X-ray centroid; Crowther et al. 2003).

Bauer, Brandt 2004

- 32 hour period, well established distance,
- bright X-ray source, X-ray eclipses

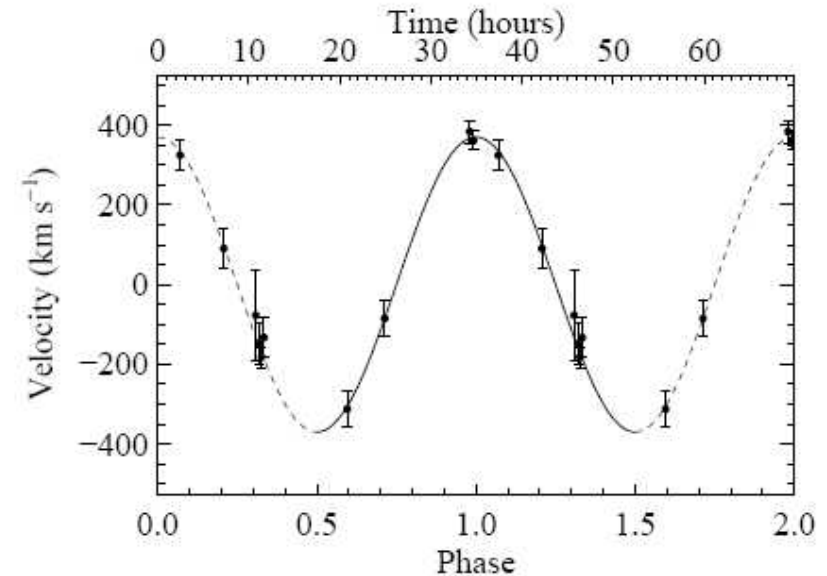


FIG. 3.— Radial-velocity curve of [MAC92] 17A using velocities relative to the [O III] $\lambda 5007$ spectral line. Two cycles are shown for clarity. Formal velocity error bars are 1σ . See the text for values of the fit parameters.

Silverman Filipenko, 2008

Parameters of IC10X-1

TABLE 2
DERIVED BLACK HOLE MASS (M_{\odot})

Inclination (deg)	Wolf-Rayet Mass (M_{\odot})		
	17	25	35
90	23.1 ± 2.1	27.7 ± 2.3	32.7 ± 2.6
78	23.9 ± 2.1	28.6 ± 2.4	33.8 ± 2.8
65 ^a	27.1 ± 2.5	32.3 ± 2.8	37.9 ± 3.2

^a If the mass of [MAC92] 17A is $35 M_{\odot}$, inclinations less than $\sim 78^{\circ}$ will not yield X-ray eclipses. Silverman Filipenko, 2008

This system survived the critical point in the evolution!

Component masses in NGC300 X-1

- Mass estimate from mass function and identification of the WR star:

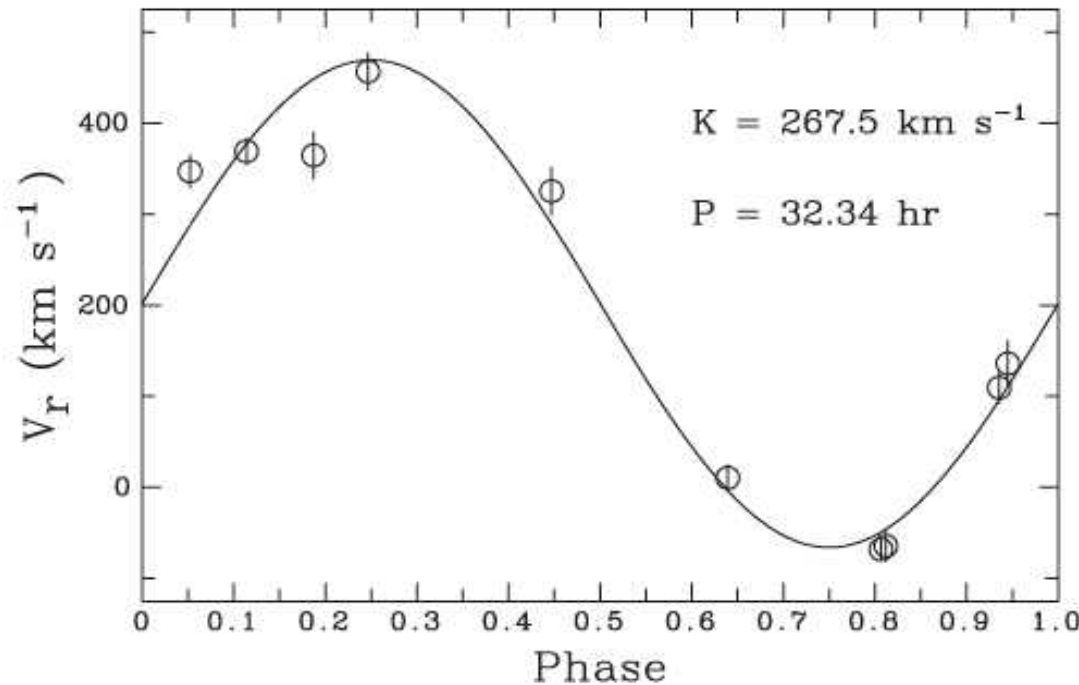


Figure 3. Radial velocity variations of $\lambda 4686 \text{ He II}$ phased to 32.3 h, from which a systemic velocity of $v_r = 202 \pm 7 \text{ km s}^{-1}$ and semi-amplitude of $K_2 = 267.5 \pm 7.7 \text{ km s}^{-1}$ are obtained.

On the spins

- Final spins of the binaries: should they be aligned?
- Binary evolution – little angular momentum transfer onto BH
- Initial spins likely unchanged, small kicks can misalign them
- In short: aligned spins point at binary origin but misaligned do not contradict it

On the spins

- In the GC model – spins randomly oriented
- In the chem homogenous model – aligned but the same caveats apply as in the case of binary evolution
-

Summary

- Standard binary evolution can explain observed properties of BBH: masses, merger times, rates.
- Need to place the scenario in the framework of other known objects: X-ray binaries, CE events, etc.
- Mass distribution hints at high number of BBH and much less binaries with NS – we should be able to use the observed mass distribution to constrain models
- Rate density should increase with z – rate increase will be a model discriminator as well

Summary 2

- Distinguishing other models
- GC – spins, also mergers with IMBHs
- Chemically homogenous model: equal mass ratios. Search for progenitor binaries.